UNIVERSIDADE DE LISBOA
FACULDADE DE CIÊNCIAS
DEPARTAMENTO DE FÍSICA

Work-related Upper Body Postures Classification and Segmentation

Diogo Canadas Sózinho

Mestrado em Engenharia Biomédica e Biofísica

Dissertação orientada por:
Prof. Dr. Nuno Matela
Dr. André Carreiro

2024

Agradecimentos

Este documento resulta de 1 ano e 4 meses de trabalho repletos de desafios e superações. De certo que o resultado de todo o esforço não seria o mesmo sem a diversa ajuda e suporte que recebi ao longo deste percurso.

O meu primeiro agradecimento dirige-se a toda a equipa Fraunhofer Portugal AICOS pelo ambiente que torna difícil entrar e sair pela porta sem aprender algo novo. Mais especificamente um obrigado aos meus orientadores André Carreiro e Lua Nunes que me introduziram ao mundo da inteligência artificial. Ao André pela incrível supervisão que tornou um percurso montanhoso bem mais direito. À Lua pelo incontestável brio, excelência e perfeccionismo com que me orientou a cada passo dado ao longo deste caminho.

Agradeço também ao meu orientador interno Professor Nuno Matela por me sugerir esta possibilidade de realizar a dissertação na Fraunhofer, assim como a prontidão de resposta e resolução de burocracias evitando que estas se tornassem problemas.

À equipa de ergonomia da Volkwagen Autoeuropa, Carlos Furjão e Natércia Domingues pelo interesse e colaboração em acrescentar uma nova dimensão a este trabalho.

Não poderia deixar de agradecer ao Nuno Bento, o meu professor de *machine* e *deep learning*, obrigado pela preocupação, orientação e amizade. Um obrigado também ao meu outro guardião de *deep learning* Pedro Matias.

Um obrigado especial aos meus amigos: Andreia, Brito, Chico, Dani, David, Leonor, Mariana, Pinela, Pipa e Toni, por festejarem as minhas vitórias e ouvirem as minhas preocupações. Não poderia pedir um grupo melhor com quem terminar esta etapa.

Um obrigado particular ao meu parceiro David que partilhava do meu horário noturno tornando as noites de trabalho menos solitárias.

Agradeço ao meu amigo Tiago Gil pelas verificações constantes no meu bem-estar e progresso, motivando-me a trabalhar e não me fazendo esquecer do que havia no fim deste percurso. Fico à espera do meu jantar bro.

A ti, Leonor, obrigado nunca será suficiente. Sem o teu apoio ainda não era desta. Obrigado pelo amor, preocupação, por me puxares para cima e por me fazeres um pouco melhor todos os dias. *Wherever you are in the world, I swear that I will find you again*.

Mãe e Pai, o vosso apoio foi essencial para a conclusão desta jornada e finalmente já está. Obrigado por me darem na cabeça e não me deixarem ser menos do que o que sou capaz. Obrigado por me darem valor, espero deixar-vos orgulhosos.

Um obrigado especial aos meus avós. Por não exigirem nada de mim, mas fazendo-me acreditar que sou capaz de tudo.

Resumo

Na União Europeia, 3 em cada 5 trabalhadores do setor industrial relatam sofrer de lesões musculoesqueléticas relacionadas com o trabalho. Ademais, lesões musculoesqueléticas correspondem a cerca de 15% do número total de anos perdidos devido a uma doença ou lesão de origem ocupacional. Este tipo de lesões são frequentemente consequência de posturas corporais extremas, movimentos repetitivos e levante e transporte de objetos pesados, sendo que afetam principalmente os membros superiores.

Com a ascensão das Indústrias 4.0 e 5.0, o cenário industrial passou por uma transformação digital significativa, visando aumentar a produtividade de maneira sustentável, com foco na saúde e no bem-estar dos trabalhadores. Neste contexto, o projeto OPERATOR surge com o objetivo de desenvolver tecnologias que facilitem o processo de avaliação da segurança de trabalho, promovendo a sensibilização para a interação entre os trabalhadores e o local de trabalho, com a finalidade de reduzir potenciais problemas de saúde.

Este propõe o desenvolvimento de uma avaliação ergonómica automática e personalizada efetuada na linha de montagem automóvel da Autoeuropa. Recorrendo à utilização de unidades de medida inerciais (IMUs) em alternativa aos procedimentos manuais utilizados atualmente. Estes dados permitem classificar posturas de trabalho e automatizar o preenchimento de formulários de avaliação de risco, como a European Assembly Worksheet (EAWS), e reportar informação da exposição ao risco baseada na norma 11226 da *International Organisation for Standardization* (ISO), suportando a tomada de decisão/intervenção dos ergonomistas.

A presente dissertação aborda dois problemas principais: classificação de posturas complexas e desenvolvimento de uma *dashboard* para suporte à prática ergonómica.

Em primeiro lugar, no âmbito da classificação de posturas que envolvem mais de uma articulação, a utilização de ângulos articulares representa um desafio complexo, uma vez que a classificação baseada somente em limites angulares revela ser insuficiente. Neste contexto, foi desenvolvido um modelo de aprendizagem profunda para classificação de posturas, com foco em posturas complexas, como posturas de trabalho com os braços ao nível dos ombros ou trabalho acima do nível da cabeça. No desenvolvimento do modelo usou-se a base de dados AnDy, pela sua semelhança com os dados da Autoeuropa ao nível das características dos mesmos, do tipo de sensores usados e das posturas registadas. Esta compreende dados de 17 IMUs adquiridos aquando da simulação de tarefas industriais típicas da fabricação automóvel, possuindo mais de cinco horas de dados adquiridos a partir de 13 sujeitos.

Adicionalmente, esta base de dados possui as posturas de trabalho devidamente anotadas segundo o EAWS. Foi utilizado o método da janela deslizante para gerar janelas de 0.5 segundos com uma sobreposição de 25% sobre os dados e respetivas anotações. As janelas resultantes contêm dados de aceleração, aceleração angular e ângulos articulares relativos aos membros superiores. Estas janelas de dados foram utilizadas no treino de quatro classificadores de *machine learning* (ML) para classificar as posturas: *decision tree*, *random forest*, *support vector machine* e *Gaussian Naïves-Bayes*. A avaliação destes modelos baseou-se no método de validação cruzada reservando-se os dados de cada sujeito à vez como

conjunto de teste durante o treino do classificador. Ademais, foi realizada otimização de hiperparâmetros através da técnica de *grid search*. Contudo, os classificadores testados apresentaram uma performance máxima de *F1-score* de 0.39 para a postura de trabalho com os braços ao nível dos ombros, revelando-se insuficientes para a realização da tarefa de classificação dado esta ser uma das duas posturas de interesse.

Deste modo, desenvolveu-se uma rede neuronal convolucional constituída por quatro camadas convolucionais 1D intercaladas com três camadas *max-pooling*, seguida de uma camada *flatten* e três camadas densas. Cada camada convolucional possui o dobro do número de filtros do que a camada convolucional anterior. Além disso, o modelo foi treinado ao longo de 100 épocas utilizando um tamanho de grupo de 16, uma taxa de aprendizagem de 0.00001, 16 filtros, um tamanho de filtro de 7, e otimizador *Adam*. A estratégia selecionada para a validação do modelo foi a validação cruzada deixando de fora cada um dos treze sujeitos e fazendo a média das métricas de avaliação. A rede supramencionada classificou as posturas em cinco categorias: em pé, curvado para a frente, fortemente curvado para a frente, mãos ao nível dos ombros, mãos acima da cabeça. Tendo em consideração as posturas que são o foco da classificação, foram obtidos valores para o *recall* de 0.95 para a classificação da postura de trabalho ao nível dos ombros e 0.97 para trabalho acima do nível da cabeça. Adicionalmente, o *F1-score* médio obtido para a classificação das cinco posturas foi de 0.96, usando 35 features. O estudo de referência atinge este mesmo valor usando 69 features.

Posteriormente, os resultados da classificação de posturas complexas são remitidos para os algoritmos de cálculo de exposição e risco ergonómico. Estes algoritmos segmentam as séries temporais, i.e., dados recolhidos com IMUs, de acordo a norma ISO 11226, e determinam as pontuações de risco segundo o EAWS.

Em segundo lugar, na Autoeuropa a avaliação de risco é atualmente um processo trabalhoso e demorado, realizado através do preenchimento do formulário EAWS. Deste modo, com o propósito de fornecer um suporte visual aos ergonomistas, desenvolveu-se uma *dashboard*. Esta ferramenta apresenta gráficos e métricas que visam facilitar e aprimorar a prática ergonómica. Na *dashboard* são apresentados os dados provenientes dos algoritmos de exposição e risco, em forma de gráficos e métricas calculadas a partir dos mesmos. Os gráficos desenvolvidos apresentam dados angulares e a sua respetiva segmentação em posturas aceitáveis e não recomendadas, segundo a norma ISO, para cada segmento corporal. Além disso, possibilitam também a segmentação segundo intervalos articulares. Esta ferramenta realiza o cálculo da percentagem de tempo de exposição a posições aceitáveis e não recomendadas, bem como o registo do número de ocorrências de exposição. Por fim, é apresentada uma tabela com a percentagem de exposição a intervalos articulares/posturas, e o valor de risco associado a um ciclo de trabalho médio e calculado segundo o EAWS, para cada postura de trabalho.

Esta *dashboard* foi desenvolvida em conjunto com dois ergonomistas da Autoeuropa, tendo sido concebida para este caso de estudo em particular.

Além de suplantar os desafios inerentes ao preenchimento trabalhoso, demorado e subjetivo do EAWS por parte dos ergonomistas, através da aquisição de dados com IMUs e a classificação automática de posturas, a *dashboard* proporciona aos ergonomistas a capacidade de conduzir uma análise mais completa através das visualizações e valores demonstrados.

Esta inclui a avaliação individual de risco, possibilitando a medição do risco relativo a um posto de trabalho para segmentos corporais específicos de um indivíduo. A análise possibilita a personalização da avaliação individual, permitindo a alocação do indivíduo a postos e rotações de trabalho que viabilizem a produtividade mesmo em condições de lesão, proporcionando benefícios tanto para o mesmo quanto para o fabrico.

O próximo passo consiste na validação do modelo com dados específicos recolhidos linha de mon-

tagem da Autoeuropa e no teste da viabilidade e usabilidade da *dashboard* com o utilizador final, neste caso, os ergonomistas da Autoeuropa. A transição dos dados de uma base de dados pública para os dados específicos do caso de estudo, é crucial para confirmar a aplicação prática e eficácia das ferramentas desenvolvidas. Além disso, a adaptação da *dashboard* para permitir uma comparação direta e automatizada entre postos de trabalho, sequências de trabalho e entre diferentes indivíduos visa potencializar e otimizar ainda mais o trabalho dos ergonomistas na prevenção de lesões musculoesqueléticas.

Palavras chave: Lesões musculoesqueléticas relacionadas com o trabalho, Reconhecimento de posturas, Análise de séries temporais, Ergonomia ocupacional

Abstract

The European Union faces a significant challenge, with three out of five industrial workers reporting musculoskeletal injuries linked to work, primarily affecting the upper limbs due to extreme postures, repetitive movements, and heavy object handling. Industry 4.0 and 5.0 have prompted a digital transformation in the industrial sector, emphasizing sustainable productivity and worker's well-being.

In response, the OPERATOR project aims to enhance work ergonomics evaluation, fostering awareness of worker-workplace interaction to mitigate potential health issues. This project involves developing an automatic ergonomic assessment for Autoeuropa's automotive assembly line, using inertial measurement units (IMUs). This automation extends to the European Assembly Worksheet (EAWS) and integrates International Organisation for Standardization (ISO) norm 11226 standards to support ergonomists decision-making.

The present dissertation addresses two key challenges: classifying complex postures and developing a dashboard for ergonomic practice support.

A deep learning model was developed to perform posture classification focusing on complex working postures, such as arms at shoulder level or overhead work. Using the AnDy dataset, which is composed of automotive industry-like tasks collected by 17 IMUs and annotated according to the EAWS, the model achieved recall values of 0.95 and 0.97 for shoulder-level and overhead working postures, respectively.

The two mentioned postures are fed into ergonomic exposure and risk determination algorithms, utilizing ISO 11226 and EAWS.

Additionally, a dashboard was co-developed with two Autoeuropa ergonomists aiding with the laborious and time-consuming risk assessment currently performed. The tool integrates data from the ergonomic exposure and risk algorithms, presenting graphs and metrics. It calculates risk exposure percentages and number of occurrences, as well as provides risk scores for five work postures according to the EAWS, ultimately enabling ergonomists to perform a more detailed, simple and personalised ergonomic risk assessment for each worker.

Keywords: Work-related musculoskeletal disorders, Posture recognition, Time series analysis, Occupational ergonomics

Graphical Abstract

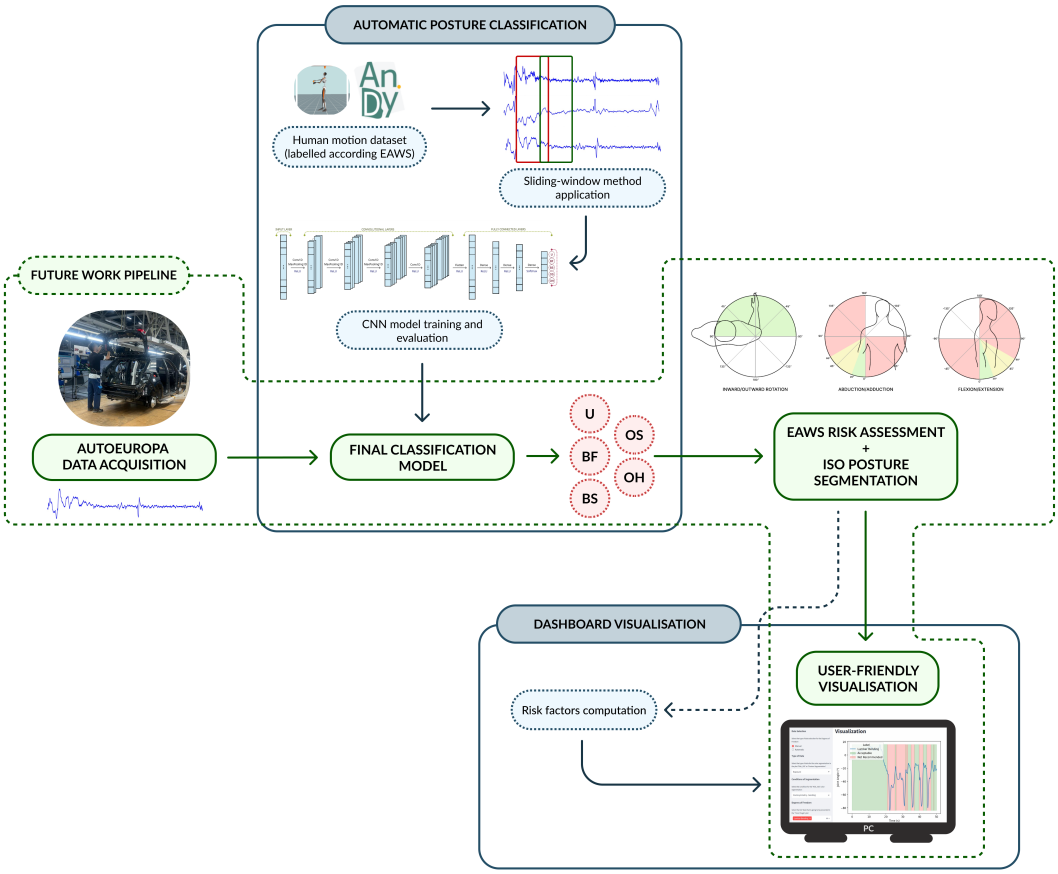

Figure 1: Graphical abstract of this dissertation.

Index

List of Figures

LIST OF FIGURES

List of Tables

Acronyms

ADL Activities of daily living. 6, 43

AI Artificial Intelligence. 21

ANN Artificial neural network. 23

AUC Area under the curve. 28

BF Bent forward. xii, 30, 33, 39, 42

BoB Biomechanics of Bodies. xi, 9, 13

BS Strongly bent forward. xii, 30, 33, 39

CM Confusion matrix. 27, 40, 41

CNN Convolutional neural network. xii, xiii, 7, 8, 26, 29, 35, 36, 39, 41, 43, 45, 54

DL Deep Learning. xiii, 6–8, 27, 41

DNN Deep neural network. xi, 23, 24

DoF Degree of Freedom. xiii, 15, 16, 31, 48–50, 52

DT Decision tree. 22, 35, 39

EAWS European Assembly Worksheet. iv, v, vii, xi–xiii, 5, 7, 19, 20, 29, 30, 32, 37, 41, 45, 49, 50, 52, 54, 66

EU-OSHA European Agency for Safety and Health at Work. 2

FC Fully connected. 26

FN False negative. 27

FP False positive. 27

GDP Gross domestic product. 2

GNB Gaussian Naïve Bayes. 22, 35, 39

GS Grid search. 22

HAR Human activity recognition. 3, 6

HMM Hidden Markov Models. 7

IEA International Ergonomics Association. 17

IMU Inertial measurement unit. iv, v, vii, xiii, 4, 6–8, 20–22, 26, 29–33, 36, 41, 52, 54

ISO International Organization for Standardization. iv, v, vii, xii, xiii, 18, 19, 29, 37, 48–52, 54, 67

LOSOCV Leave-one-subject-out cross-validation. 34, 35, 39, 44

LSTM Long short-term memory. 7, 8, 43

LSTM-RNN Long short-term memory-based recurrent neural network. 7, 8

ML Machine learning. iv, xiii, 6–8, 21–23, 27, 32, 33, 35, 41, 44, 54

MoCap Motion Capture. 6, 20, 30

MSD Musculoskeletal disorder. 2, 14, 18, 46

NN Neural network. xi, 23, 24

OAWS Ovako Working Posture Assessment System. 5

OCRA Occupational Repetitive Action. 5

OH Overhead work. xii, xiii, 30, 33, 39–45

OS Shoulder level work. xii, xiii, 30, 33, 39–45

REBA Rapid Entire Body Assessment. xi, 9, 13

ReLU Rectified linear unit. 25, 35

RF Random forest. 7, 8, 22, 35, 39, 40

ROC Receiver operating characteristic. 28

ROM Range of motion. xi, 15–17

RULA Rapid Upper Limb Assessment. 5, 6, 9

SVM Support vector machine. 6–8, 22, 35, 39, 40

TN True negative. 27

TP True positive. 27, 28

TSFEL Time Series Feature EXtraction Library. xiii, 33, 34

U Upright. xii, 30, 33, 39, 42

WRMSD Work-related musculoskeletal disorder. xiii, 1–3, 6, 8, 14, 18, 45, 52, 54

WRULMSD Work-related upper limb musculoskeletal disorder. 2, 3

Chapter 1

Introduction

1.1 Problem

Work-related Musculoskeletal Disorders (WRMSDs) are a group of disorders that affect the musculoskeletal system, such as muscles, tendons, and nerves. These health conditions are perpetuated from the constant repetition of motions and awkward postures commonly found in industries, such as in automotive assembly lines [1, 2].

The main risk factors associated with WRMSDs are related to the work activity in itself, intrinsic to the worker, or related to organisational/psychosocial factors, detailed in Table 1.1 [3]. Exposure to these factors is directly related to the risk of developing WRMSDs. However, the effects of being exposed to these factors become more nefarious with increasing duration, frequency and intensity of exposure [3].

Table 1.1: Risk factors contributing to the development of WRMSDs

Related to Work	**Intrinsic to the Worker**	**Organisational/Psychosocial**
Extreme Body Postures/Positions	Age	Intense work rhythms
Force Exertion	Gender	Monotony of tasks
Repetitiveness	Anthropometrics Measures	Insufficient social support
Mechanical Elements Exposure	Health Status	Organizational production model

WRMSDs cause pain, discomfort, and disability, being responsible for lowering the worker's overall quality of life, while also harming companies and societies, leading to decreased productivity and increased healthcare costs, respectively [4]. Enhancing working conditions in the industrial sector is crucial for mitigating WRMSDs. Several methods have been developed to perform risk assessment and can be divided into self-reported, observational or direct measurements methods [5].

This thesis addresses the issue of WRMSDs and risk assessment in the context of the Volkswagen Autoeuropa automotive industry to aid ergonomics professionals in assessing workers' risk so they can be a positive force in attenuating the hazards workers are subjected to. In Volkswagen Autoeuropa assembly lines, risk assessment is performed resorting to specific proforma sheets filled by the ergonomics specialists who perform their evaluations by direct observation or video recordings of the workers. This method demonstrates a restrained level of personalization for each worker, is not very accurate, is time-consuming and the data is difficult to extract since manually assessing the repetitiveness and overall exposure to certain risk postures is no easy task.

1.2 Motivation

In pursuing global sustainability and development, the United Nations outlined several key objectives addressing diverse socio-economic and environmental challenges. Some of these following objectives intersect with the work being developed in the context of this dissertation [6]:

- the 8^{th} objective focuses on decent work and economic growth, which poses challenges for integrating scalable ergonomic solutions in the workplace;
- the 9^{th} targets industry, innovation, and infrastructure, which requires industry development and adaptation to sustain efficient production while focusing on the workers' well-being.

With the emergence of Industry 4.0, we have witnessed the digitalization of industrial processes, marked by the integration of digital technologies into the industrial apparatus and procedures. This shift aims to streamline operations, improve efficiency, and increase productivity, culminating in the development of a smart factory [7]. Furthermore, Industry 5.0 is a newly developed concept that supplements Industry 4.0, following a human-centric approach. Industry 5.0 is all about positioning the workers back at the very centre of the fabrication process allowing for sustainable human-machine collaboration committed to supporting the workforce [8, 9].

According to a report by the European Agency for Safety and Health at Work (EU-OSHA) of 2019 ([10]), approximately, three in every five workers in the European Union express complaints related to musculoskeletal disorders. Additionally, among all workers who experienced work-related health problems, 60% reported having musculoskeletal disorders (MSD). Besides the great number of people affected by MSDs in the workforce, these disorders also add up to 15% of the total years of life lost due to disease or occupational injury. Particularly, in the automotive assembly industry, workers are prone to the development of MSDs just like in any other industry. However, a set of additional elements specific to this sector adds to the risk for MSDs. As stated in a study conducted in an automotive assembly line in Iran [11], the workforce of an automotive manufacturing line is susceptible to the accelerated rhythm of the production process, repetitive movements, awkward postures, lifting and moving of heavy objects and extended periods standing which collectively exacerbate the risk of MSDs.

WRMSDs also have negative impacts on an economic level. In 2016, Germany disclosed a loss of 30.4 billion euros of gross value added which represents roughly 1% of the country's gross domestic product (GDP). Additionally, as stated by [12], the economic burden associated with MSDs amounts to €240 billion in Europe, which is equivalent to up to 2% of the GDP.

With this in mind, preventive measures such as equipment to help with lifting or moving heavy objects, task rotation for repetitive movements, and regular work breaks, among others, have shown efficacy. As reported by EU-OSHA, 31% of workers express backaches in countries and sectors with five to six preventive measures implemented on average, versus 51% in countries and sectors where only one to three measures were adopted [10].

According to the authors of [13], a study on MSD complaints performed in Portugal that involved 515 companies and 410 496 workers, upper limb injuries are the most predominant lesions in the automotive assembly industries. Moreover, according to the authors of [14], assembly lines, in addition to being environments susceptible to the development of WRMSDs, are especially prone to such issues affecting the upper limbs. As mentioned previously, work's repetitiveness, limited recovery interval, and physical strain are some of the risk factors for the development of MSDs. In an assembly line context, these aspects are difficult to overpass, resulting in a high rate of manifestation for work-related musculoskeletal upper limb disorders (WRULMSDs). Furthermore, these conditions rapidly progress to a chronic

state, largely because the diagnosis is hard to ascertain since most instances are only identified after a second episode, i.e., acute pain episode [15, 16]. Given this information, the early detection of musculoskeletal discomfort and continuous health monitoring are crucial steps in avoiding the development of WRULMSDs and ensuring workforce health [14].

1.3 Context

Prevention of WRMSDs carried out by ergonomics specialists involves different approaches that face several challenges. Usually, ergonomics experts resort to observational methods to examine the work methods in terms of posture, employing established guidelines/standards to perform evaluation. This time-consuming approach involves abundant manual data collection, preventing frequent individualized data gathering [17]. Furthermore, these observations entail one extra challenge since the worker is aware that his work method/posture is being examined, leading to the collection of biased data.

This dissertation was developed under the scope of the OPERATOR project. With the advent of the Internet of Things, this project grounds the opportunity to set the worker's health as the central piece of the digital transformation in the industrial and service sectors. [18]. Volkswagen Autoeuropa is a collaborating member within the consortium of this project, serving as the case study of automotive assembly line.

This dissertation proposal focuses on applying human activity recognition (HAR) to ergonomics, addressing the need to implement models to recognize and analyze postures across workers, and assess work-related risk factors [19]. Additionally, it aims to enhance data access and analysis for the ergonomics experts team responsible for the design and optimization of the work environment to ensure the worker's safety and well-being. This enhancement culminated in developing a dashboard specialized in the use case of the Autoeuropa ergonomics team.

1.4 Objectives and Research Questions

The main goal of this dissertation is to develop an automatic risk assessment tool tailored for the ergonomics team at Volkswagen Autoeuropa, in order to assist them in the optimization and personalization of the workplace for every worker. The objectives and research questions that support this work are presented in Table 1.2.

Table 1.2: Research questions and objectives for the present dissertation.

Research Questions	Objectives
Can the application of machine learning and deep learning models effectively classify upper body postures in the context of industrial tasks?	Recognition of complex worker's upper body postures using data collected from IMUs
Can posture classification be performed for complex upper body postures solely using IMU data?	
How to effectively preprocess IMU data to perform posture classification?	
What information and metrics help the ergonomists the most to assess a worker's risk?	Associate worker's posture detection with injury risk assessment in automotive assembly line workers
What are the best ways to present visual information about a worker's posture to the ergonomist?	Develop a dashboard to help ergonomists visualize and analyse a worker's exposure to ergonomic risk

1.5 Structure

The present document is divided into six chapters:

1. Introduction - introduces the problem and context that raised the issue to investigate;
2. State of the Art - addresses the latest research studies for risk assessment, posture classification and ergonomic evaluation on automotive assembly lines, as well as risk assessment visualisation;
3. Theoretical Background - presents the scientific background behind this dissertation;
4. Materials and Methods - exhibits the materials used and the methods behind this dissertation's approach;
5. Results and Discussion - showcases the obtained results and their analysis;
6. Conclusion and Future Work - concludes the work on the most relevant outcomes and suggests the next steps regarding the topic of study.

Chapter 2

State of the Art

2.1 Automotive Industry Ergonomics

2.1.1 Tools for Upper Body Posture Exposure and Risk Evaluation

There are various methods to perform risk assessment for physical loads and these can be categorized as self-reported, observational, and directly measured [5]. Self-reported methods comprise questionnaires, interviews, and workers' diaries. This method for risk assessment is considered to be inaccurate since it is derived from the worker's capability to estimate their physical load which can easily tend to be under or overestimated. Moreover, these evaluations are frequently conducted post-work, relying on memory, which could introduce recall bias, affecting the accuracy and volume of memories due to subsequent events [20]. Observational methods bridge these constraints. They consist of proforma sheets (i.e., checklists) filled in by an observer and have multiple dimensions related to exposure to physical risk factors, providing a score on the workstation risk. Optical observational methods are also more advanced observational techniques that can be integrated with biomechanical models of the worker's body to extract more relevant information about workers' postures and physical load. Nevertheless, proforma sheets are susceptible to variability induced by the observer, and videos demand both higher costs and technical support [5, 17]. Several proforma sheet methods used in observational ergonomic risk assessment are listed below based on [17], [5] and [21]:

- Ovako Working Posture Assessment System (OAWS) - Facilitates a comprehensive risk assessment by observing body postures and considering the weight of the load in use;
- Rapid Upper Limb Assessment (RULA) - Allows the classification of postures and force based on the deviation of each separate body segment from a reference neutral position;
- Occupational Repetitive Action (OCRA) - Applied across various professions, it assigns a numerical risk score based on factors like repetition, force, awkward postures, and other relevant considerations;
- European Assembly Worksheet (EAWS) - Developed specifically for the automotive industry use case, enables analyses using different parameters, for example, working postures, forces, manual materials handling and repetitive loads.

Another method to perform risk assessment emerged to overcome the time-consuming and biased results through direct measurements. These enable extensive and accurate data gathering to further biomechanical, cardiopulmonary, muscular, and psychophysical assessments. In-field direct measurements are

employable with a difficulty level equivalent to an expert using an observational method [5, 17]. Furthermore, the authors of [22] showed that wearable devices, such as inertial measurement units (IMUs), are a better fitting approach for on-site ergonomic risk assessment than markerless optical technology.

2.2 Posture and Activity Classification

Observational methods used in conventional risk assessment are time-consuming tasks that require manual annotation of workers' postures from a field expert and posterior analysis. Besides, significant variability in the scoring accuracy is dependent on the observer's subjective judgment and expertise. To overcome this challenge, motion capture systems (MoCaps) have been used as a way to collect data and develop semiautomatic approaches either through optical, or IMU-based motion capture to evaluate risk using direct measurements [5, 23, 24].

The authors of [25] and [26] developed methods to evaluate the risk of developing WRMSDs using optical motion capture. The first created a computer vision approach that analyses videos of workers engaged in industrial tasks to automatically estimate exertion time, duty cycle, and hand activity level. The second employed a vision-based method to perform a real-time posture assessment by calculating the RULA activation level, i.e., a metric to help determine the urgency and severity of ergonomic issues.

Optical MoCaps systems offer exceptional precision but pose challenges due to their high cost, dependence on technical expertise, and susceptibility to environmental factors like illumination, occlusion, or complex scenes. Consequently, these limitations render them impractical under certain work conditions [24, 27].

When it comes to the classification of activities and postures using direct measures, several methods have been developed over the years. The authors of [28], [29] and [30] extensively reviewed human activity recognition research works in the context of classification of activities of daily living (ADL), which comprises standing, walking, falling and many others. Several of these studies employ IMUs for data collection, incorporating both machine learning (ML) and deep learning (DL) methodologies for classification. ML and DL are complex models that are further explained in sections 3.4 and 3.4.4, respectively. Some of these methods are presented in Table 2.1 alongside methods for posture classification.

Moreover, the sliding window approach serves as a widely adopted preprocessing technique in (HAR) as it is direct and effective in categorizing periodic activities. This method can employ a fixed or variable window size, with or without overlap, however, it is crucial to ascertain optimal parameters. A window size too small might fragment a single activity into two, while an overly wide size may encompass two or more activities [31]. In alignment with the authors of [32], the recommended window size for activity recognition involving the upper body (trunk and arms) is between 1 and 4.5 seconds, offering optimal recognition performance. Additionally, a minimum window size of 0.5 to 1.25 seconds is identified as sufficient for achieving reasonable performance.

Table A.1 presents a brief description of the datasets used in the study by the authors of [33], [34] and [35]. The H-Activity, MHEALTH, UCI-HAR, WISDM, and OPPORTUNITY datasets consist of data related to ADL. In contrast, the Skoda dataset comprises actions specific to a car maintenance scenario, such as opening the hood or closing the trunk. It's important to note that in these datasets, acceleration data is consistently collected, while angular velocity data is present in five out of the six datasets. Additionally, UCI-HAR, H-Activity, and WISDM datasets utilize smartphones for data acquisition, while MHEALTH, OPPORTUNITY, and Skoda datasets employ wearable sensors.

Firstly, the authors of [36] perform posture classification by employing a support vector machine (SVM), a machine learning (ML) classifier, to distinguish between safe and unsafe postures based on

kinematic parameters estimated from a biomechanical model created from the implementation of inertial measurement units (IMUs). The authors of [37] achieved accuracies of 93% to 98% for static and dynamic activities classification also resorting to ML approaches, namely, random forest (RF) and SVM. This study required the use of only one accelerometer placed on the chest to perform such classifications.

Secondly, the authors of [33], [34] and [35] resort to more advanced ML approaches, using deep learning (DL) approaches combining convolutional neural networks (CNNs) and long short-term memory (LSTM) networks to perform activity recognition on the mentioned datasets. Moreover, the authors of [38] use a long short-term memory-based recurrent neural network (LSTM-RNN) to predict seated postures with accuracy and an F1-score of 99.0% and 96.6%, respectively. These networks take into account the sequence of the data being very used in activity recognition. Nevertheless, concerning the working posture classification problem in this dissertation, the temporal aspect of the data is not as relevant.

Hence, the primary focus will be on the study conducted by the authors of [39]. In this research, the AnDy dataset ([40]), which encompasses industry-like tasks, was used for classifying actions and postures using Hidden Markov Models (HMM) based on postures assessed in the EAWS. Notably, this dataset aligns with the one employed in the present dissertation. The study explored different sets of activities and postures for recognition, as well as various subsets of features. The proposed method achieved a global F1-score of 91.55% when classifying the postures corresponding to the torso and arms configuration (upright, bent forward, strongly bent forward, shoulder level work and overhead work). It's worth mentioning that, similar to LSTM networks, HMM is employed for sequential data, being initially employed in the study for activity recognition, and subsequently applied to posture classification.

Table 2.1: Studies that used machine learning (ML) or deep learning (DL) approaches to classify actions and postures.

Reference	Task	Sensors	Method
[33]	Activity classification using 3 datasets: H-Activity, MHEALTH and UCI-HAR	Wearable sensors and smartphones	Deep CNN-LSTM model with self-attention
[34]	Activity classification using 3 datasets: UCI-HAR, WISDM and OPPORTUNITY	Wearable sensors and smartphones	Deep neural network that combines convolutional layers with LSTM
[35]	Activity classification on the Skoda and OPPORTUNITY datasets	Wearable sensors	DeepConvLSTM model that comprises convolutional, recurrent and softmax layers
[36]	Distinguish between safe and unsafe postures using the tasks: a lifting load task using the correct and incorrect postures and a releasing load task also using the correct and incorrect postures	Eight IMUs (Xsens) placed on the chest, pelvis, the mid-thighs, the mid-shanks and the instep of the feet.	SVM classifier trained on kinematic parameters estimated from a biomechanical model
[37]	Classification of 4 static activities: standing erect, standing with the trunk bent forward, left, or right. And 7 dynamic activities: trunk twisting, lateral bending and flexion/extension, squatting, slow walking, fast walking, and running.	One accelerometer placed on the chest	Two classifiers were tested: Random Forest (RF) and Support Vector Machine (SVM)
[38]	Seated posture classification: Upright, Slump, Lean, Right bending, Left bending, Right twisting, Left twisting	Four 9-axis IMUs distributed uniformly between T1 and L5	Time-domain features served as inputs for a long short-term memory-based recurrent neural network (LSTM-RNN)
[39]	Classification of postures and actions related to 6 tasks: screw low, screw middle, screw high, untie knot, carry 5kg and carry 10kg (AnDy dataset)	Xsens motion capture suit and e-glove	Hidden Markov Models and wrapper-based methods for automatic feature selection

2.3 Ergonomics Evaluation Interfaces

2.4 Visualisation

The development of ergonomic risk assessment tools has gained recent attention to mitigate the incidence of WRMSDs in the workplace. There is a growing demand for ergonomic risk management tools that not only identify ergonomic risks but also support proactive responses to these risks [41].

Existing approaches to automated assessment vary in terms of the used feedback mechanisms, while some advocate for immediate alerts to workers upon detecting awkward poses through means of vibration or visual signals, others compute risk scores and depict them over time in graphical formats that are subsequently analyzed by ergonomists [42].

A universal requirement exists for effective visualisation of ergonomic data, specifically for tools that integrate both visualisations and numerical data (for example, automatic filling of proforma sheets) to enhance ergonomic risk assessment. Visual tools contribute to enhancing the understanding of the current ergonomic situation for both workers and ergonomists, facilitating the creation and adjustment of workplaces [41, 43].

The authors of [43] focus on developing an interactive visualisation tool tailored to enhance the work evaluation process for ergonomists. In a practical test involving an ergonomic risk assessment task, the results demonstrated that this tool empowered both ergonomists and non-experts to identify highly critical problems, recognize periods with an elevated frequency of such issues, and precisely locate specific occurrences, including their timing and location. Therefore, the significance of interactivity becomes evident as a crucial feature for effective visualisation, particularly when dealing with intricate results that demand thorough analysis and adjustments to multiple parameters. Interactive visualisation tools provide ergonomists with the capability to actively engage with the data, facilitating the manipulation of parameters and exploration of information from diverse perspectives and levels of detail.

2.4.1 Commercial Available Solutions

At present, ergonomic risk assessment involves the use of traditional proforma sheets, which are filled in by professionals who observe workers in the course of their tasks [39, 44]. Besides being laborious and time-consuming, these methods are also prone to the observer's subjectivity, leading to biased conclusions.

Considering this challenge, various tools have been created to improve the risk assessment process by enhancing the visualisation of information, such as:

- SoterTask is a tool developed by SoterAnalytics that supports ergonomic assessments using a video of the worker. This tool creates a report based on the Rapid Entire Body Assessment (REBA) worksheet [45];
- inSEER is a software that resorts to a video taken from a worker executing a task to perform a report showing the worker's exposure to risk postures [46];
- ergoIA software requires a video of a worker to identify specific postures executed during the recorded work [47];
- ErgoPlus is an ergonomic management software that allows for risk assessment, improvement planning and progress tracking [48];
- The Biomechanics of Bodies (BoB) developed BoB/Ergo, an analysis system that joins a human musculoskeletal model to an interface capable of calculating several worksheet scores, such as REBA and RULA, and other data such as joint ranges of motion or muscles forces [49].

An example of SoterTask's interface is shown in Figure 2.1 to illustrate the types of data and the varieties of visualisations possible.

As illustrated in Figure 2.1, SoterTask's software facilitates the visualisation of angle plots for specific body segments over a designated timeframe. The plot incorporates colour segmentation, with green indicating low risk, yellow denoting medium risk, and red signalling high risk based on predefined angular limits. Additionally, the software provides a percentage breakdown of time spent under high, medium, or low ergonomic risk. The software's capability to segment data for the back, neck, right and left arms, as well as the right and left legs is also a relevant feature.

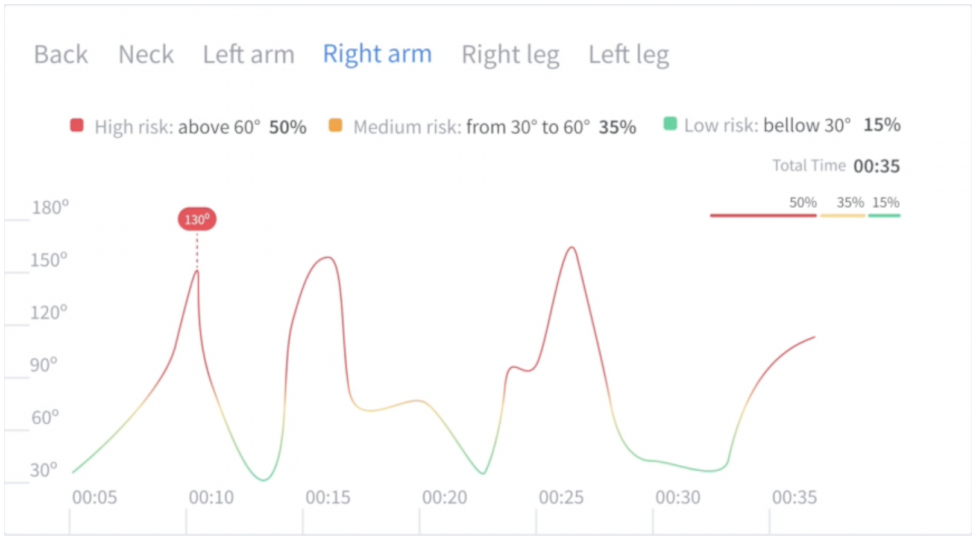

(a)

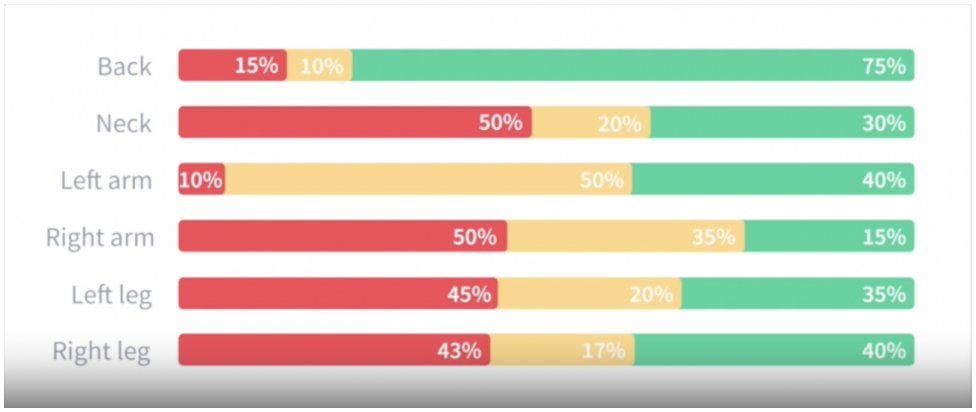

(b)

Figure 2.1: Example of visualisation possible with the SoterTask software. (a) presents an angle from the right arm over time signalled with high, medium or low ergonomic risk. (b) shows the overall exposure, per body segment, to risk

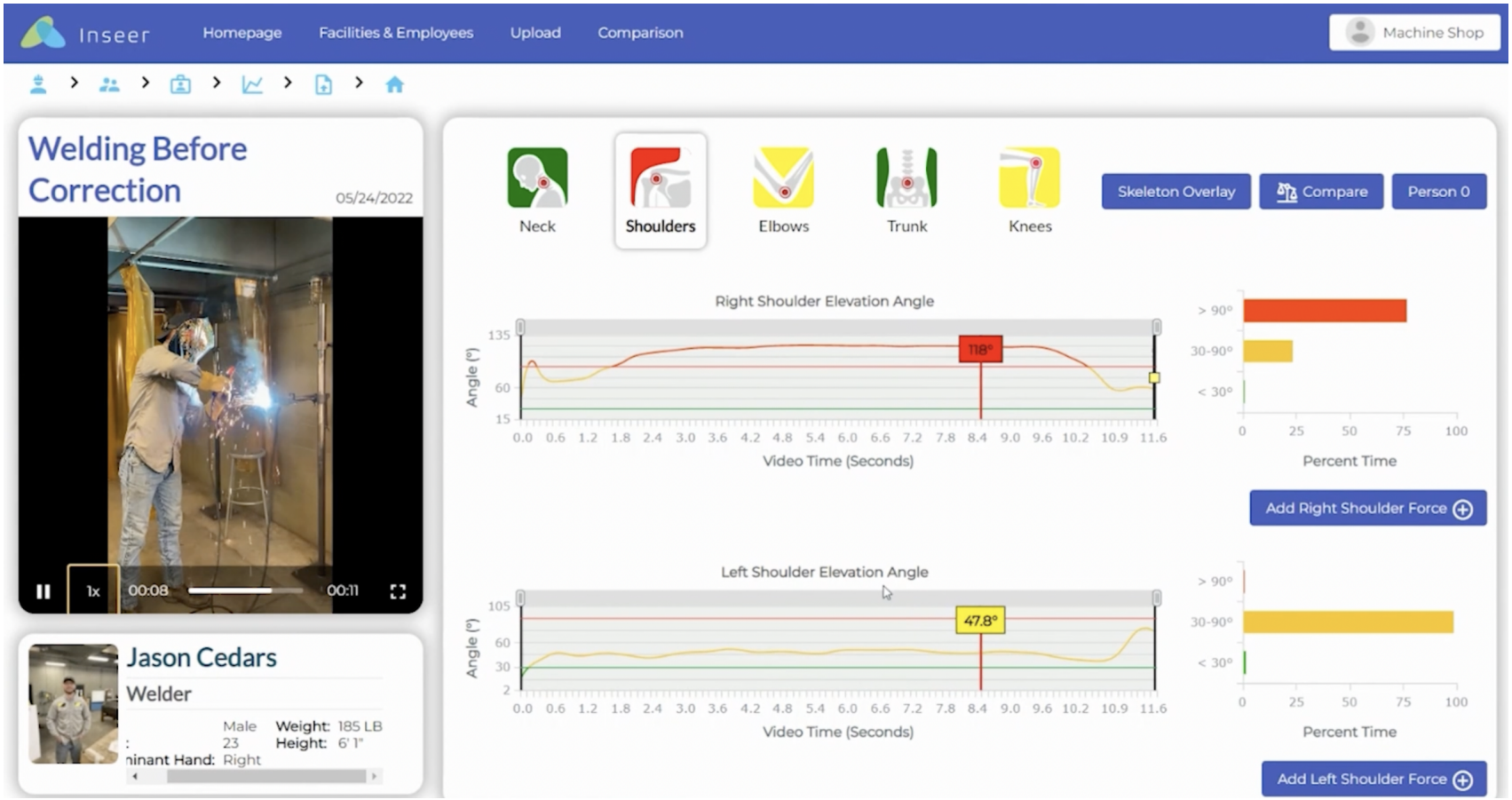

Figure 2.2: Inseer software interface with an example of visualisation for the shoulders' data.

The inSEER software, depicted in Figure 2.2, features a line plot illustrating the angle variations over time for the neck, shoulders, elbows, trunk, and knees. Similarly to Sotertask, it also provides a bar chart indicating the percentage of time spent in specific angular positions, with colours green, yellow, and orange representing progressively higher angles (below 30º, between 30º and 90º, and above 90º, respectively). Additionally, the software includes a video presentation synchronized with the visualized data, as well as additional details about the worker.

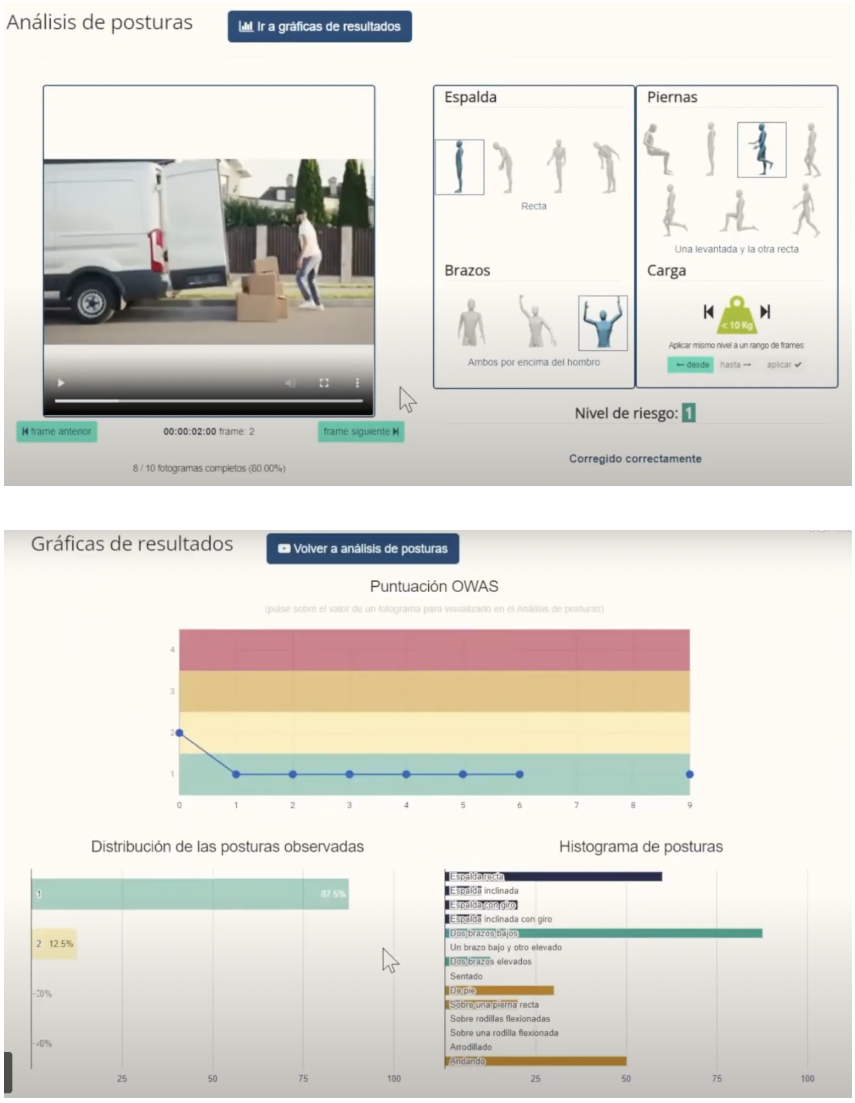

Figure 2.3: Example of visualisation possible with the ergoIA software. (a) presents a video and the posture selection interface. (b) shows data related to the presence of the selected posture.

Similarly to Sotertask and Inseer, ergoIA also conducts its analysis automatically utilizing a worker's video. As presented in Figure 2.3, the software visually represents the worker's posture concerning the trunk, arms, and legs, synchronizing each frame of the video. Additionally, it incorporates risk assessment by computing the Ovako Working Posture Assessment System (OWAS) scores for the analyzed video. The analysis is further complemented by a bar chart illustrating the percentage of time a worker spends in various postures (e.g., both arms elevated) or activities (e.g., walking).

The ErgoPlus software presented in Figure 2.4 enables the simultaneous analysis and management of multiple workstations. Notably, the software features a human body representation where each body segment is highlighted with a distinct colour corresponding to the level of risk exposure.

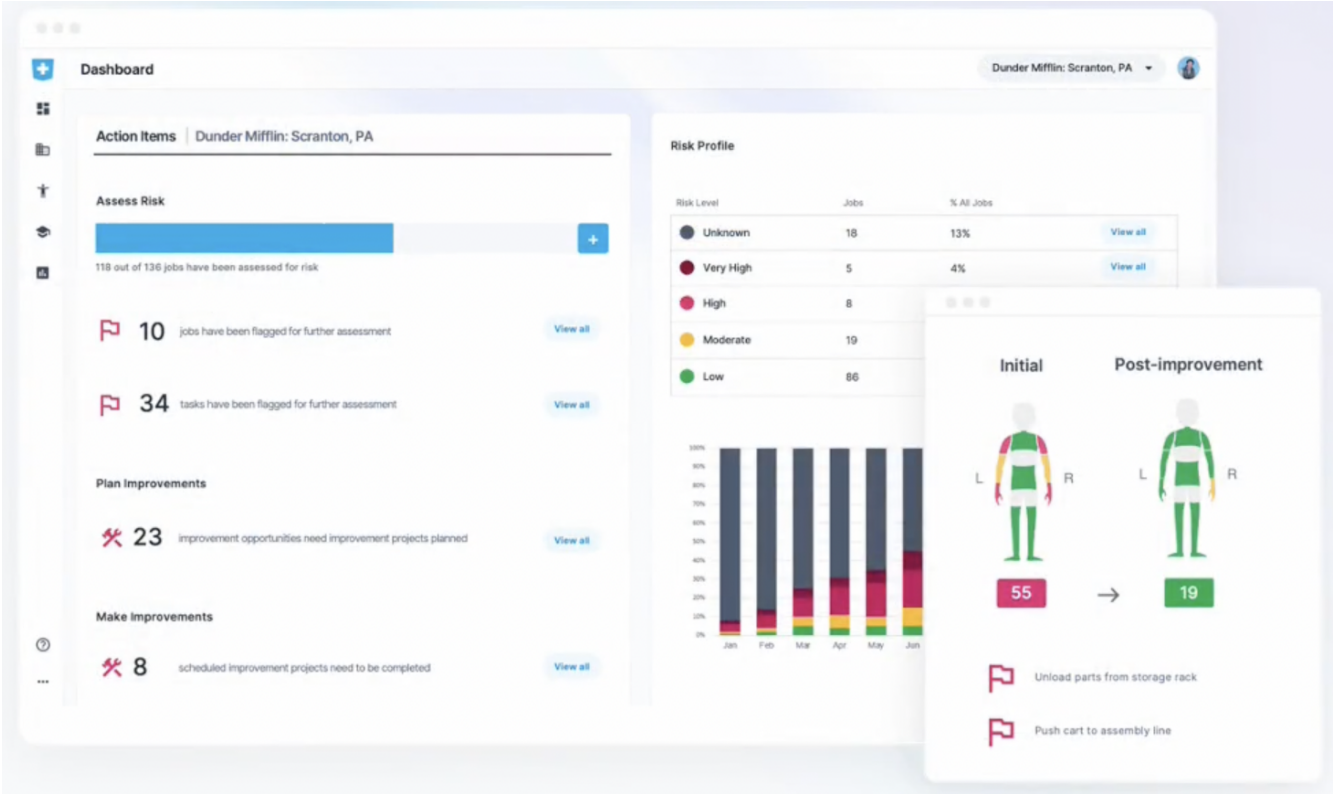

Figure 2.4: Example of the ErgoPlus software with a general risk profile for each job and a body scheme signalling the most risk for each body segment.

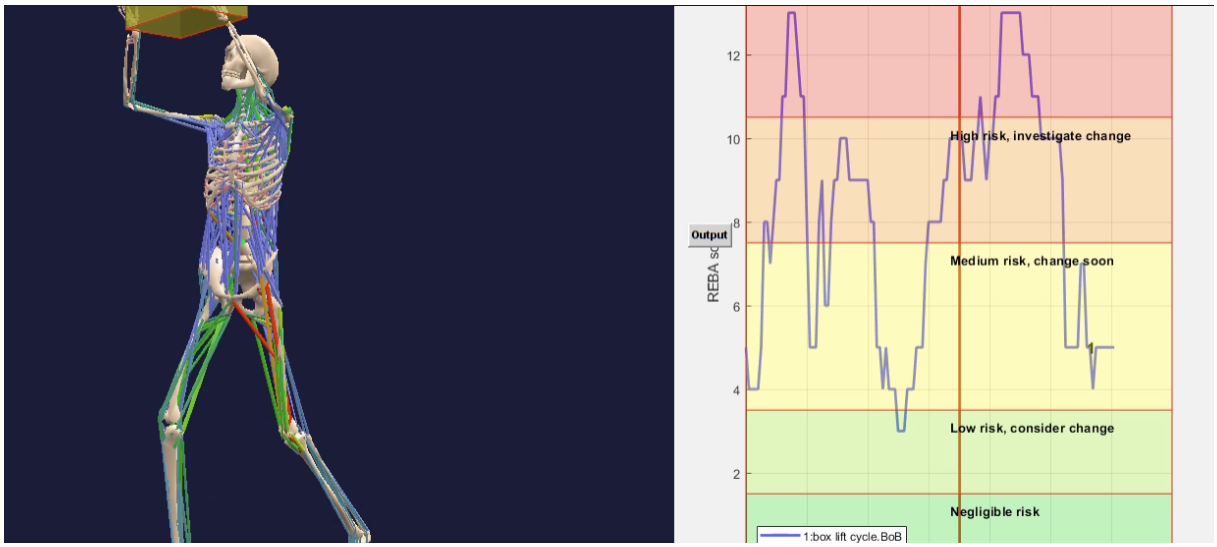

Figure 2.5: Example of visualisation using the BoB software. This example presents a human musculoskeletal model and the REBA score updated over time.

BoB serves as a biomechanical modelling software presenting a human musculoskeletal model and allowing diverse analyses. This model can be directly integrated with acquisition systems, such as the Xsens MVN Analyze. Figure 2.5 exhibits a graph illustrating the REBA score over time, featuring distinct colour segmentation for straightforward identification of periods with different risk levels.

Chapter 3

Theoretical Background

3.1 Work-related Musculoskeletal Disorders

Musculoskeletal disorders are chronic pain syndromes that encompass a range of conditions affecting the musculoskeletal system, specifically targeting muscles, tendons, and nerves. When MSDs occur in occupational contexts, they are referred to as WRMSDs. Examples of common upper body WRMSDs are presented below [1, 3]:

- The rotator cuff tendinitis, among the most prevalent shoulder pathologies, arises from maintaining the upper limbs elevated at or above shoulder level, from repetitive elevation, or even from performing circular arm movements while elevated;
- The carpal tunnel syndrome is identified as a neuropathic injury involving compression of the median nerve within the confined space of the carpal tunnel, located in the wrist. Hyperflexion and hyperextension of the wrist contribute to the onset of this WRMSD;
- Wrist tendonitis or tenosynovitis can be induced by repetitive flexion/extension motions of the wrist, even when executed with the manipulation of light loads, or when sustaining a load in an awkward posture;
- Lateral epicondylitis, commonly known as tennis elbow, is a tendinopathy that arises due to the overuse of the elbow joint through repetitive movements. Medial epicondylitis, also referred to as golfer's elbow, is also a tendinopathy that develops in response to the overuse of the handling of excessive or unevenly distributed loads;
- Rachialgias are the most frequently reported concerns associated with occupational activities. Among the most prevalent complaints are lower back pain and neck pain. Possible contributors to spinal pain include sustained standing postures, repetitive flexion and extension of the spine, manual handling and transportation of loads, and prolonged sitting while working with a computer;

3.2 Human Motion

Initially, to understand and describe human movements, it is fundamental to comprehend the anatomical description of the human body. This description starts with dividing the body according to 3 anatomical planes: frontal (or coronal), sagittal and transverse. Motion within a specific plane takes place through rotation around an axis positioned at a 90º angle to that plane, so for the frontal, sagittal and transverse

anatomical planes, the correspondent axes are the anteroposterior, the mediolateral and the longitudinal axis, respectively [50]. Figure 3.1 presents a graphical representation of the mentioned anatomical planes and axes.

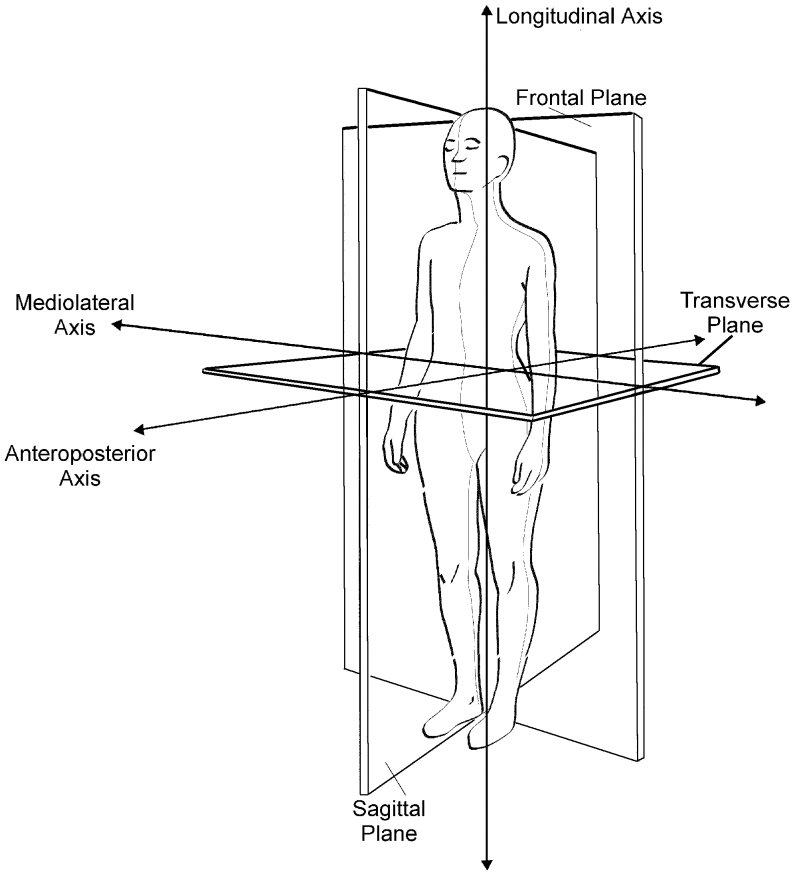

Figure 3.1: Anatomical planes and anatomical axis [50].

Furthermore, major bones united through joints define body segments. The rotation of these segments around the anatomical axes can be described using specialized terms [50]:

- Flexion specifies the decrease in the joint angle (angle formed by two body segments) around the mediolateral axis in the sagittal plane, while extension refers to the increase of the joint angle. Note that movements that exceed the range of motion (ROM) of the joints during the actions of flexion and extension correspond to hyperflexion and hyperextension, respectively;
- Abduction describes a body segment's movement away from the midline in the frontal plane. On the contrary, adduction is the movement of a body segment towards the midline in the frontal plane;
- Inward and outward rotation can be defined as the rotation around the longitudinal axis of the body segment toward and away from the body's midline, respectively.

As this dissertation focuses on upper body movements, the motions of the spine as well as the joints from the shoulder, elbow and wrist are explained further in detail below with a visual representation of the degrees of freedom (DoF) and the ROM for each joint's motion. Figure 3.2 illustrates the spine's DoF that enables the trunk's motions of lateral bending, rotation and extension/flexion along with the ROM for each movement.

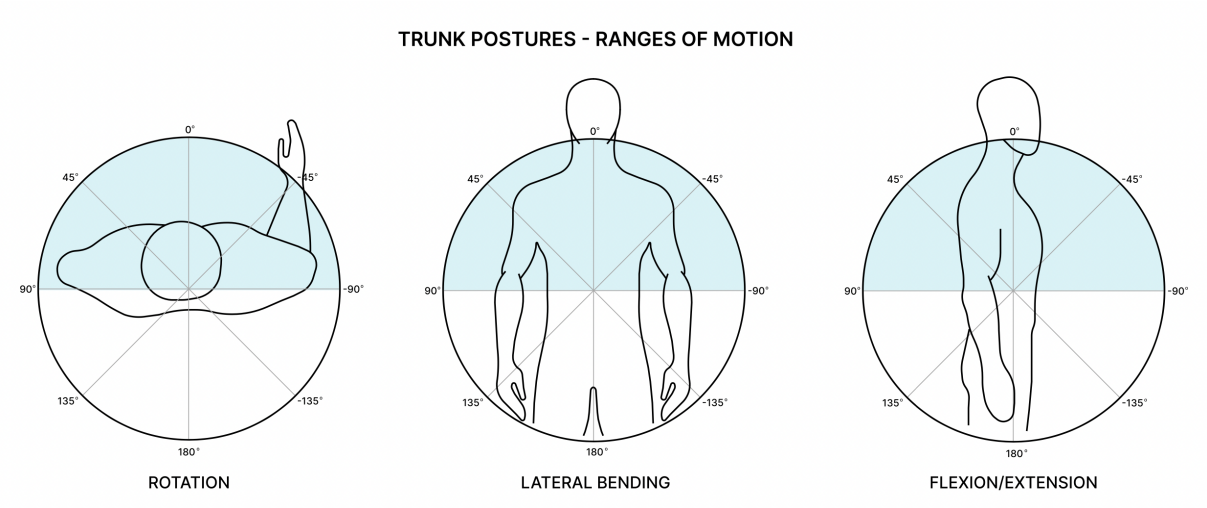

Figure 3.2: Spine lateral rotation (left), bending (middle) and flexion/extension (right). These postures have a ROM between -90º and 90º (adapted from [51]).

Figure 3.3 displays the shoulder's DoF that enables the motions of abduction/adduction, flexion/extension and inward/outward rotation, along with the shoulder's ROM for each movement.

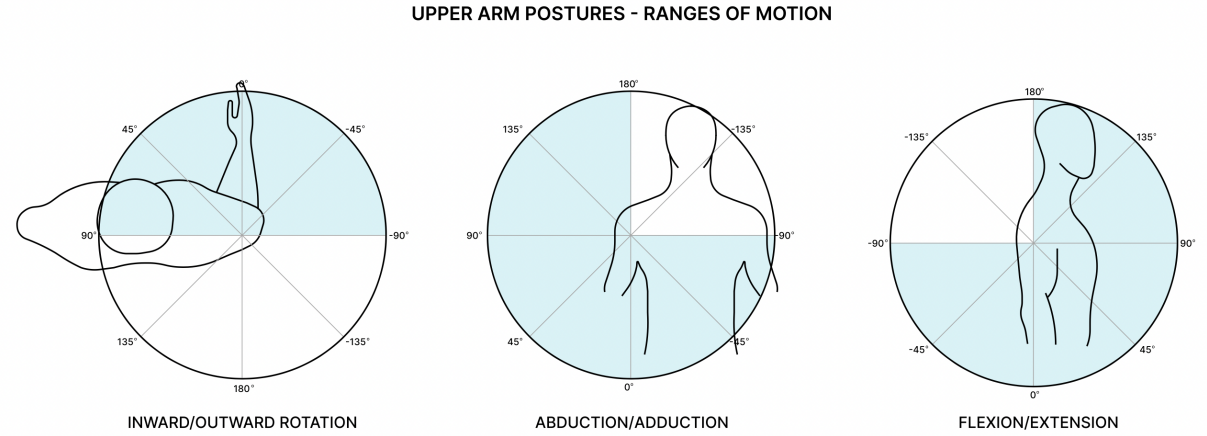

Figure 3.3: Shoulder inward/outward rotation with ROM between -90º and 90º (left), shoulder abduction/adduction with ROM between -90º and 180º (middle) and shoulder flexion/extension with ROM between -90º and 180º (right) (adapted from [51]).

Figure 3.4 is related to the elbow's flexion/extension and pronation/supination along with the forearm's ROM for each movement. Finally, Figure 3.5 exhibits the wrist's DoF of flexion/extension and ulnar/radial deviation and the hand's ROM for each movement.

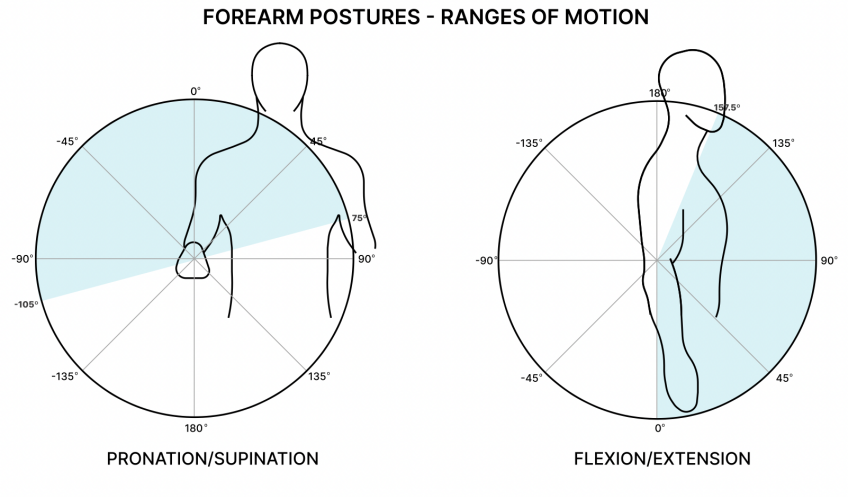

Figure 3.4: Elbow pronation/supination with ROM between -105º and 75º(left) and elbow flexion/extension with ROM between 0º and 157.5º (right) (adapted from [51]).

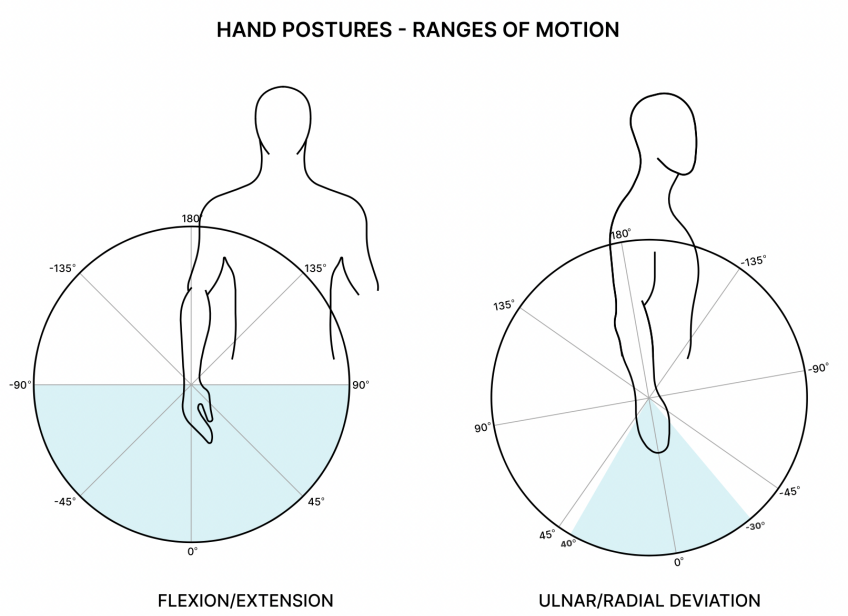

Figure 3.5: Wrist flexion/extension with ROM between -90º and 90º (left) and ulnar/radial deviation with ROM between -30º and 40º (right) (adapted from ([51]).

3.3 Ergonomics

Ergonomics derives from the Greek *ergon* meaning work and *nomos* meaning law, and refers to the study/science of work [52, 53]. Ergonomics is defined by the International Ergonomics Association (IEA) as "the scientific discipline concerned with the understanding of interactions among humans and other elements of a system, and the profession that applies theory, principles, data, and methods to design to optimize human well-being and overall system performance" [54].

Therefore, ergonomics advocates for a comprehensive and human-centred approach to the design of work systems, with the main goal of establishing a workplace environment that maximizes the health and well-being of the workers, while also boosting the organization's productivity and efficiency [53, 55].

3.3.1 Components of Ergonomics Evaluation

With this in mind, it is up to the ergonomists to play the vital role of shaping and assessing tasks, roles, products, environments, and systems to ensure they align with the requirements, capacities, and constraints of the workers [53]. Hence, there are several factors to consider that shape workplace ergonomics [55, 56]:

- Physical factors, such as the repetitiveness and the intensity (handled weight) of the work;
- Cognitive factors, such as task variability and difficulty;
- Organizational factors, such as teamwork;
- Environmental factors, such as the noise or temperature the worker is exposed to.

Examples of physical factors in the industrial setting are (1) the physical workloads the worker is subjected to by lifting or carrying heavy objects, (2) awkward postures, (3) task repetitiveness and (4) exposure to vibration, for example by operating tools [57]. This dissertation focuses on the physical ergonomic factors that contribute to exacerbating upper body WRMSDs in the context of automotive assembly lines, more specifically in upper body awkward postures.

3.3.2 Posture Evaluation

As previously indicated, uncomfortable postures constitute a primary factor contributing to WRMSDs, particularly in industrial settings such as automotive assembly lines [2]. Unfavorable work conditions may induce prolonged work under improper posture, which in turn lead to pain, fatigue and MSDs. Musculoskeletal pain and fatigue can, in turn, impact posture control, increasing the likelihood of errors and leading to diminished work quality, production efficiency, and the potential for hazardous situations [51].

3.3.2.1 ISO 11226

To assess static working postures and offer appropriate protection for nearly all healthy adult workers, the International Organization for Standardization (ISO) introduced "ISO 11226:2000" [51]. This International Standard establishes ergonomic guidelines for various work tasks by defining recommended thresholds for static working postures taking into consideration body angles and temporal aspects.

ISO 11226 determines the acceptability of static working postures categorizing them into "Acceptable" and "Not Recommended" based on body angles and dependent on the posture holding time, i.e., the time the postures are maintained.

Table 3.1 presents shoulder and upper arm postural acceptability according to ISO 11226 for awkward upper arm postures, upper arm elevation, and shoulder raise, characterizing each posture into "Acceptable" (postures with no risk associated), "Not recommended" (risky postures), or "Dependent on holding time" (postures can be classified either "Acceptable" or "Not recommended" depending on the holding time). In Table 3.1, awkward upper arm posture refers to upper arm retroflexion (elbow positioned behind the trunk when observed from the side of the trunk), upper arm adduction (the elbow is not visible when observed from the back of the trunk), or extreme upper arm external rotation (outward rotation around the longitudinal axis of the upper arm relative to the trunk over 90°). Upper arm elevation is the difference of flexion or abduction between the static working posture and the reference posture.

Table 3.1: Shoulder and upper arm postures' acceptability (adapted from ISO 11226) [51].

Postural characteristic	Acceptable	Dependend on holding time	Not recommended
Awkward upper arm posture			
No	X		
Yes			X
Upper arm elevation			
> 60º			X
20º to 60º without full arm support		X	
20º to 60º with full arm support	X		
0º to 20º	X		

3.3.2.2 European Assembly Worksheet

The EAWS is a risk assessment tool developed to conduct holistic risk assessment in the context of the automotive industry. This proforma sheet consists of five sections. Firstly there is a general section, followed by specific sections focusing on "working postures", "action forces", "manual material handling", and "repetitive upper limbs movement" [21, 58]:

- The general section provides general insights into the assessment to be conducted, offering a comprehensive evaluation of the analyzed task or workstation. This includes considerations about additional physical workloads, time aspects for repetitive loads of the upper limbs, among other relevant aspects;
- The working posture section conducts evaluations for static working postures and frequent high-movement activities. Symmetrical working postures, such as bending forward or above shoulder level work, are assessed in various positions, including standing, sitting, kneeling, and others. Additionally, asymmetric effects, such as trunk rotation, lateral bending, and far reach, are also taken into account;
- The section on action forces assesses forces exceeding 30-40 N for both the entire body and the hand-finger system, addressing force exertions intensity, duration and repetition;
- The section on manual materials handling encompasses loads exceeding 3–4 kg, taking into account multiple factors, including the weight of the loads, the working postures associated with handling, the working conditions, the frequency and the duration of the handling tasks;
- The repetitive movements for the upper limbs section consider factors such as the intensity and frequency/duration of applied forces, gripping conditions, upper limb postures, and various additional elements, including rest pauses and exposure to cold or vibration;

As this dissertation focuses on the postural behaviour of the workers, the focus will be on the "working postures section", since it is the one related to standing (and walking) upper body postures and, therefore, the most relevant for the developed work. Figure 3.6 shows the selected section "Basic Positions/Postures and movements of trunk and arms (per shift)" of EAWS emphasizing the "Standing (and walking)" portion.

By examination of EAWS's portion presented in Figure 3.6 it is possible to understand how the posture assessment is performed according to the proforma sheet. For every posture considered, there is a risk score associated with the duration of the position over the considered period for the assessment

Ergonomic Assessment Worksheet V1.3.3

Basic Positions / Postures and movements of trunk and arms (per shift) (incl. loads of <3 kg and action forces of 30-40 N) Static postures: > 4sec High frequency movements: 2 trunk bending or 10 arm lifting > 60° per min			Evaluation of static postures and/or high frequent movements of trunk/arms. Duration [sec/min] = duration of posture(s) x 60 / cycle time										Sum of lines	Postures: Asymmetry effects		
														Trunk Rotation 1)	Lateral Bending 1)	Far Reach 2)
		[%]	5	7,5	10	15	20	27	33	50	67	83		int 0-5 / dur 0-3	int 0-5 / dur 0-3	int 0-5 / dur 0-2
		[sec/min]	3	4,5	6	9	12	16	20	30	40	50		Intensity x Duration	Intensity x Duration	Intensity x Duration
		[min/8h]	24	36	48	72	96	130	160	240	320	400				
Standing (and walking)																
1		Standing & walking in alteration, standing with support	0	0	0	0	0,5	1	1	1	1,5	2				
2		Standing, no body support (for other restrict. see Extra Points)	0,7	1	1,5	2	3	4	6	8	11	13				
3		Bent forward (20-60°)	2	3	5	7	9,5	12	18	23	32	40				
		with suitable support	1,3	2	3,5	5	6,5	8	12	15	20	25				
4		Strongly bent forward (>60°)	3,3	5	8,5	12	17	21	30	38	51	63				
		with suitable support	2	3	5	7	9,5	12	18	23	31	38				
5		Upright with elbow at / above shoulder level	3,3	5	8,5	12	17	21	30	38	51	63				
6		Upright with hands above head level	5,3	8	14	19	26	33	47	60	80	100				

Figure 3.6: EAWS's "Basic Positions/Postures and movements of trunk and arms (per shift)" section. Here is presented the "Standing (and walking)" portion of the section relative to postures and movements of the trunk and arms.

(hereupon denominated as the work cycle). Hence, the higher the time spent on a posture during the work cycle (i.e. posture duration), the higher the associated risk score. Additionally, it is essential to acknowledge that distinct postures entail varying levels of intensity. Consequently, postures associated with higher intensities are assigned higher risk scores. Furthermore, the duration of each repetition for a certain posture is cumulative over the work cycle within the EAWS. This implies that numerous repetitions of a specific posture contribute to an increased overall time spent in that posture, consequently yielding a higher risk score.

3.3.2.3 Direct Measurements

The majority of MoCap systems employed in industrial workplace ergonomics use wearable IMUs [59, 60, 61].

To facilitate the assessment of body segment position and orientation, these instruments leverage tri-axial accelerometers and gyroscopes to determine the 3D acceleration and angular velocity of the sensor with respect to gravity. Moreover, magnetometers may be integrated to capture information about the geomagnetic field, allowing estimation of the sensor's heading about Earth's magnetic polarity. Figure 3.7 shows example plots of data acquired by an accelerometer, a gyroscope and a magnetometer of a subject standing upright, retrieved from the AnDy dataset [40].

IMUs can be employed under various configurations and numbers to estimate position, orientation and 3D rotation [62]. Joint motion can also be estimated from the usage of two inertial sensors simultaneously, for example, in the work of the authors of [63] the knee flexion angle was estimated using the difference in the rotation around the longitudinal axis of two sensors placed in the thigh and in the shank [62, 64].

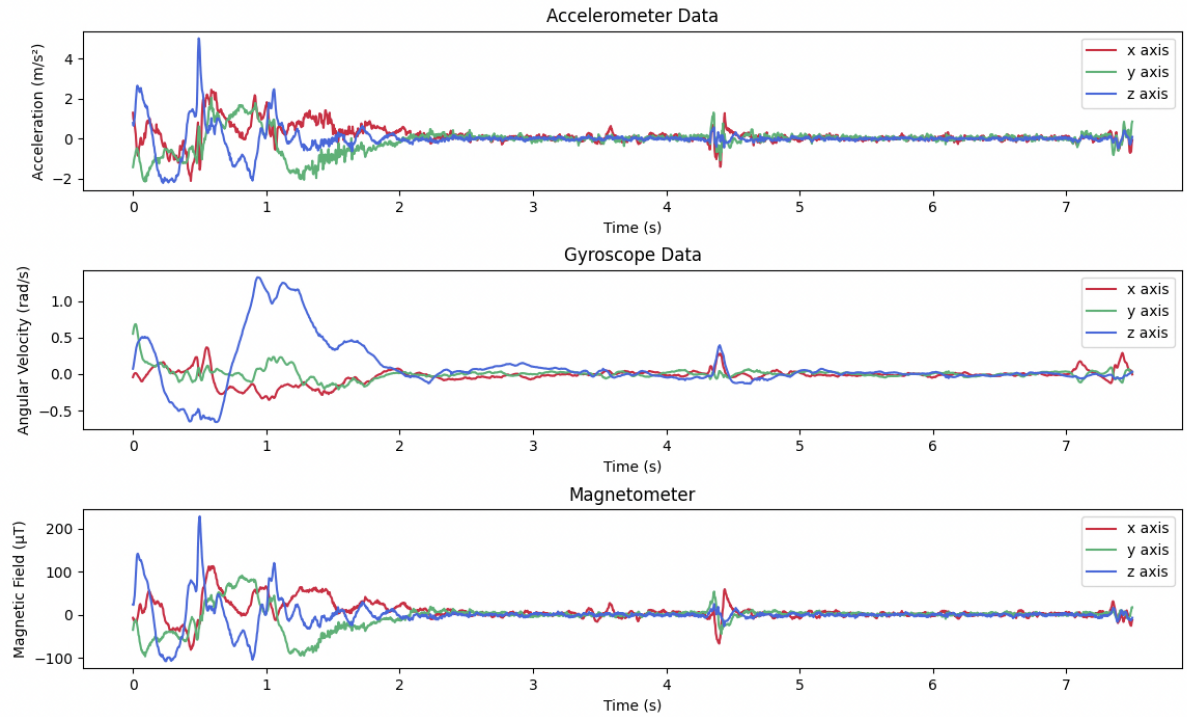

Figure 3.7: Plots of x-, y- and z-axis data of accelerometer, gyroscope and magnetometer placed on the right shoulder of a worker standing upright. Data was acquired from the AnDy dataset [40].

3.4 Machine Learning

Artificial intelligence (AI) is a field encompassing the simulation of human intelligent behaviours through computational models. As a pivotal branch of AI, machine learning entails the progressive learning of computers from examples, data, and experiences, with the ultimate goal of enhancing their capacity to manage and analyze information efficiently. ML utilizes algorithms to unveil complex relationships within vast datasets, enabling computers to autonomously discern patterns, make informed decisions, and even predict real-world events [65, 66, 67].

3.4.1 Time-series

When dealing with time series data, particularly from IMUs (as exemplified in Figure 3.7), the selection of windows is a crucial step. The sliding window method stands out as a widely adopted approach, particularly effective for recognizing periodic and static activities like walking and standing, respectively. In the sliding window technique, signals are partitioned into multiple windows of either fixed or variable sizes, with the option of allowing overlapping between these windows or maintaining distinct separation [31, 32].

3.4.2 Algorithms

Machine learning algorithms can be separated into 3 categories according to the type of learning used:

- Supervised learning requires a labeled dataset, known as the training set to predict target values by iteratively adjusting its parameters based on both correct and incorrect outputs. The training

process continues until a satisfactory reduction in error (measured by a loss function)is achieved [68];

- Unsupervised learning involves working with an unlabelled dataset to learn patterns from the data without specific guidance on a predetermined response [69];
- Semi-supervised learning leverages a combination of weak labels, or a limited labelled dataset, along with more extensive unlabeled datasets to address both supervised and unsupervised learning objectives, hence mitigating the dependency on labelled data, enabling the model to benefit from the insights garnered through unlabeled data [70, 71].

ML models can be applied to analyze time series of data such as the ones acquired with IMUs as evidenced in Figure 3.7. To perform classification using ML models, features need to be extracted from the time series of data, and supervised learning methods are the ones used to search for known patterns in the data. Some of the most used supervised ML models are:

- Decision trees (DTs) adopt a tree structure to facilitate decision-making based on conditions and their corresponding outcomes. These models acquire knowledge through a hierarchical arrangement of if/else questions centred around specific features, ultimately leading to a decision [72, 73].
- A random forest (RF) is essentially an ensemble of decision trees slightly different from the others. The underlying concept is that by constructing numerous trees, each adept at predicting in distinct ways, averaging the results leads to mitigating overfitting, enhancing the model's robustness and generalizability [73].
- Support vector machine (SVM) strives to identify a decision surface that maximizes the distance from any data point, intending to enhance classification accuracy, robustness, and generalization capability. SVM principles extend to address nonlinear problems, and also multiclass classification [74].
- The Gaussian Naïve Bayes (GNB) algorithm operates on the assumption that each feature is independent, assigning equal importance to every feature for prediction purposes. This algorithm is rooted in the principles of probabilistic classification, utilizing Bayes' Theorem [75, 76].

These models learn from the features given to them, however, there are some parameters intrinsic to the model in itself that also need to be tuned. These are called hyperparameters and cannot be directly estimated from data learning and must be set before training because they define the model architecture.

Achieving an optimal hyperparameter configuration is a crucial aspect of constructing an ML model and is commonly referred to as hyperparameter tuning. This process is particularly vital for the development of effective machine learning models, especially when dealing with tree-based models and deep neural networks that involve a substantial number of hyperparameters influencing the model's configuration.

One widely employed technique for hyperparameter optimization is Grid Search (GS). This method is known for its effectiveness and is considered an exhaustive or brute-force approach. GS systematically evaluates all possible combinations of hyperparameters within a user-defined grid configuration. This method evaluates the best hyperparameter combination by using a metric such as accuracy, for example [77].

3.4.3 Validation

In machine learning, validation methods are used to evaluate the model performance.

A simple method used is the hold-out validation where the data is divided into training and test datasets (typically 80% for training and 20% for test). The training dataset represents the data used to train the model and the test dataset refers to the data used to evaluate the final model previously trained on the training dataset. The validation dataset is a data sample used for model evaluation and hyperparameter tuning that is also used before evaluating the model on the test dataset.

One other often used method for validation in ML is k-fold cross-validation. In this technique, the entire dataset is split into a k number of folds of equal size, where each fold at a time is used as the test data with the rest of the dataset as the training data. By thorough model training and testing, using each one of the k-folds as the test dataset once the k-fold cross-validation method evaluates the model by calculating the mean of each fold results [78].

3.4.4 Deep Learning

Delving further into machine learning, artificial neural networks (ANNs) emerge as the foundation of deep learning. These networks are designed to mirror the organizational structure of neurons in the human brain. A key characteristic of artificial neural networks lies in their ability to adapt internal parameters by exposure to numerous examples, maximizing learning without the need for direct specification of all parameters, which is a clear advantage against ML models.

3.4.4.1 Artificial Neural Networks

Artificial neural networks consist of layered nodes, with each node functioning similarly to a neuron in the brain. These neurons receive input signals directly from the dataset or the neurons located in the preceding layers of the neural network (NN).

In an artificial neural network, the initial layer, referred to as the input layer, receives the training data, and the hidden layer engages in calculations, ultimately generating a response through the output layer.

3.4.5 Network Training

An ANN with two or more hidden layers is defined as a deep neural network (DNN), the more hidden layers a network has, the higher its complexity and computational cost. Figure 3.8 illustrates an example of a DNN with 2 hidden layers [79, 80, 81].

After receiving inputs from neurons in the preceding model layer, a neuron computes the sum of each signal (x_j), multiplied by its corresponding weight (w_j), and incorporates the bias term (b), leading to Equation 3.1 where Z represents the weighted sum of the inputs.

$$Z = \left(\sum_{j=1}^{n} x_j w_j \right) + b \tag{3.1}$$

Subsequently, an activation function (a), a non-linear operation, is applied, resulting in the output (y) of a neuron as expressed in Equation 3.2. This process is illustrated in Figure 3.9 below [82].

$$y = a(Z) = a\left(\left(\sum_{j=1}^{n} x_j w_j \right) + b \right) \tag{3.2}$$

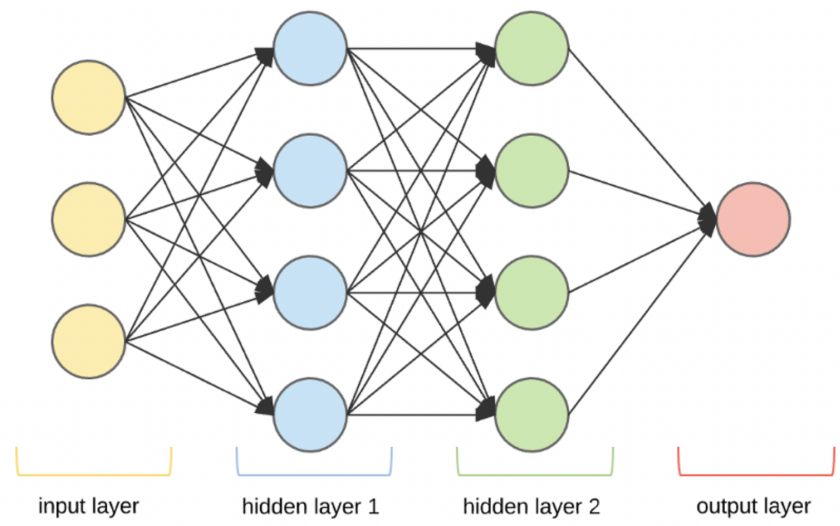

Figure 3.8: Representation of a Deep neural network (DNN).

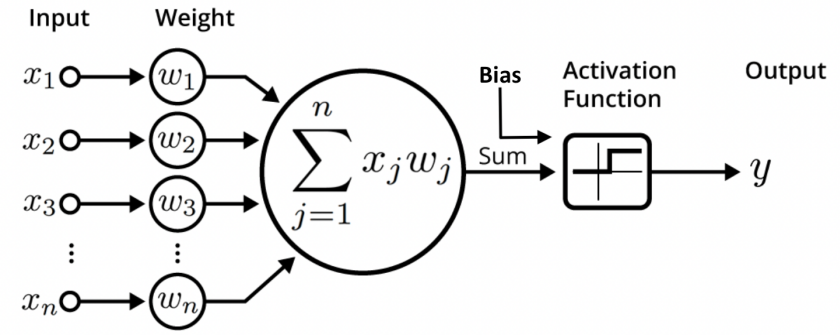

Figure 3.9: Representation of the operations inside a neuron in a NN(adapted from [80]). All the inputs are multiplied with the respective weights and summed together. The bias term is then added to the previous sum and multiplied by an activation function, resulting in the output of that neuron.

The neuron's output is then fed as input to the subsequent neuron in the next layer until it reaches the final layer where its output is used as the solution for the problem. This process is called forward propagation.

Upon reaching the output layer and producing a response, the model engages in a comparison between the generated solution and the ground-truth values sourced from the training dataset. This iterative process, commonly recognized as backpropagation, calculates the gradient of the network's error for each parameter. Through backpropagation, the model gains insights into how the parameters should be adjusted to minimize the error value.

The model undergoes training on a batch-by-batch basis, with the batch size determining the number of samples used for learning during each iteration. This batch size defines the quantity of training dataset samples processed by the model in a single learning cycle. Each complete passing through the entire training dataset, one batch at a time, is called an epoch.

The training process starts with feeding a batch of data into the input layer, followed by its progression through the hidden layers until reaching the output layer, as detailed in subsection 3.4.5.

After this, the network evaluates the output error via a loss function, comparing the output value computed by the network with the ground-truth value from the training dataset. Post error computation, the algorithm derives the error gradient along each network connection, initiating from the output layer and extending to the input layer. This enables the model to discern the influence of each connection's

weight and bias term on the outcome. This process is applied backwards through the network, therefore being called backpropagation. Ultimately, with this information, the model executes a Gradient Descent step, updating the parameters of each connection according to the previously calculated gradients [83].

There are several hyperparameters to optimise regarding network training. The learning rate is one of these hyperparameters that regulates the magnitude of the weights update as it controls the error of the loss function used for updating the model's weights [84]. Selecting an appropriate learning rate is essential since a learning rate too small finds the loss function minimum more easily, but might fall into local minimums, besides the training process is slow. Conversely, an overly large learning rate facilitates a faster learning process but may struggle to converge into the loss function global minimum[85].

An alternative to stochastic gradient descent for updating network weights is the Adam (adaptive moment estimation) optimization algorithm. Adam combines the Adaptive Gradient Algorithm (AdaGrad) with the Root Mean Square Propagation (RMSProp). AdaGrad addresses sparse gradient problems by maintaining an individual learning rate for each parameter, while RMSProp adjusts individual learning rates based on recent average magnitudes of the gradients associated with the weights.[86]

3.4.5.1 Activation Functions

As presented previously, activation functions are used to perform diverse calculations between neurons in consecutive hidden layers or from a hidden layer to the output layer. Some of the most commonly used activation functions are the Rectified Linear Unit (ReLU) and the Softmax functions.

The ReLU activation function is the most widely used activation function for deep learning applications. Operating on a threshold mechanism, this activation function sets values below zero to zero, as defined by Equation 3.3.

The Softmax activation function is used for multi-class models where it computes the probability distribution of each class, designating the target class as the one with the highest probability. This function is computed as presented in Equation 3.4, and is commonly implemented in the output layers of deep learning architectures [87].

$$y = max(0,x) = \begin{cases} x_i, \text{ if } x_i \geq 0 \\ 0, \text{ if } x_i < 0 \end{cases} \tag{3.3}$$

$$y = \frac{exp(x_i)}{\sum_j exp(x_j)} \tag{3.4}$$

3.4.5.2 Loss Functions

The loss function plays a critical role in training as it assesses the disparity between the expected value from the output and the desired value derived from the training dataset. The objective during training is to minimize this loss. Various loss functions exist, and cross-entropy loss is a commonly applied loss function that in multiclass classification scenarios, is called categorical cross-entropy. In multiclass classification scenarios, the categorical cross-entropy rises through the use of a softmax activation coupled with a cross-entropy loss. This configuration yields an output vector that signifies the probabilities of the data belonging to each considered class (from the softmax), however, only the most probable class retains the value of 1, while the probabilities for other classes are set to 0 [88].

3.4.5.3 Convolutional Neural Networks

Convolutional neural networks (CNNs) play a pivotal role in deep learning, finding extensive applications in various domains, including object tracking and action recognition. Additionally, These networks automatically generate profound features from raw data through convolution and pooling operations, proving effective in tasks such as time series classification [89, 90].

Typically, CNNs are structured with the following components:

- Convolutional layers containing sets of kernel (filters) that systematically pass across the input, performing element-wise multiplication between filter weights and input values. Notably, filter dimensions do not exceed those of the input [91, 92];
- Pooling layers, positioned between consecutive convolutional layers, employ maximization or averaging functions for data downsampling, thereby reducing parameter count [89];
- Fully connected (FC) layers receive flattened inputs from the final pooling or convolutional layer, organizing them into a vector [92];
- The nonlinearity layer, serving as the last FC layer, functions as the loss layer, computing penalties based on the discrepancy between the desired output and the calculated result [89].

Moreover, IMU data only have one dimension, therefore, as it is the input data for this dissertation, the focus will be on 1D CNNs such as the one represented in Figure 3.10.

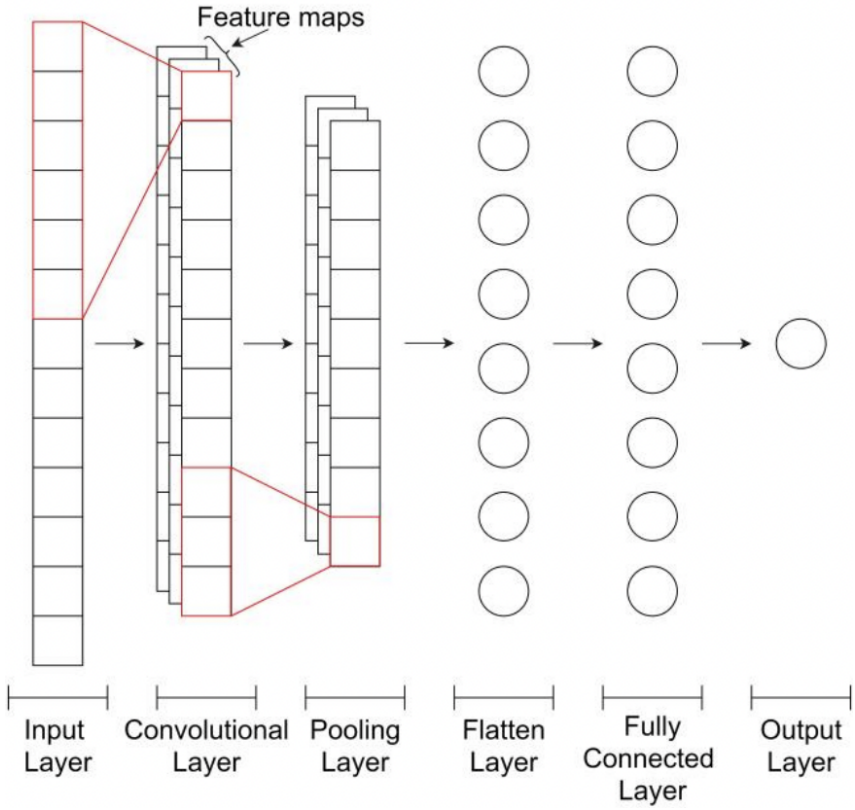

Figure 3.10: 1D convolutional neural network general architecture for time-series (from[93]).

3.4.6 Evaluation Metrics

Both ML and DL techniques resort to measurement tools to assess the performance of the model. Various evaluation metrics are employed to scrutinize distinct characteristics of the classification algorithm, providing insights from the outcomes. The assessment of model performance often hinges on accuracy, although this may be inadequate when dealing with imbalanced data, therefore deciding appropriate evaluation measures can be intricate, as each metric offers unique insights into diverse aspects of the algorithms.

In binary classification scenarios, evaluation metrics necessitate a trade-off between true positives (instances correctly classified as the positive class) and true negatives (instances correctly classified as the negative class). The evaluation metrics for multiclass problems undergo slight modifications to encompass all classes in the assessment results [94, 95].

A confusion matrix (CM) allows the visualisation of the number of instances of the positive and negative classes correctly (TP and TN, respectively) and wrongly (FP and FN) classified, this is evidenced in Table 3.2.

Table 3.2: Confusion matrix for binary classification.

		Predicted	
		Positive	Negative
True	Positive	TP	FN
	Negative	FP	TP

For multiclass classification problems, the CM is altered to incorporate multiple classes. By analysing the confusion matrices in Table 3.3, and focusing on the CM for class 'B' classification we note that TP is the number of instances the class is correctly classified as 'B', TN is the number of instances the other classes 'A' and 'C' are correctly classified, FP is the number of instances the 'A' and 'C' classes are wrongly classified as 'B', and FN is the number of instances the 'B' class is wrongly classified as 'A' or 'C'.

Table 3.3: Confusion matrices for each one of the 3 classes 'A', 'B' or 'C'.

CM for class A

		Predicted		
		A	B	C
True	A	TP	FN	FN
	B	FP	TN	TN
	C	FP	TN	TN

CM for class B

		Predicted		
		A	B	C
True	A	TN	FP	TN
	B	FN	TP	FN
	C	TN	FP	TN

CM for class C

		Predicted		
		A	B	C
True	A	TN	TN	FP
	B	TN	TN	FP
	C	FN	FN	TP

Several commonly used evaluation metrics can be extracted from the information contained in the previous confusion matrices [94, 95].

Accuracy is the ratio of correct predictions over the total number of instances evaluated. The averaged accuracy for multiclass classification is calculated using the sum of accuracy for each of the N classes.

$$\text{Accuracy} = \frac{\text{TP} + \text{TN}}{\text{TP} + \text{TN} + \text{FP} + \text{FN}} \tag{3.5}$$

$$\text{Averaged Accuracy} = \frac{1}{N} \sum_{i=1}^{N} \frac{\text{TP}_i + \text{TN}_i}{\text{TP}_i + \text{TN}_i + \text{FP}_i + \text{FN}_i} \tag{3.6}$$

Sensitivity or recall is the ratio of positive instances correctly classified within all the positive in-

stances. The averaged sensitivity for multiclass classification is calculated using the sum of sensitivity for each of the N classes.

$$\text{Sensitivity} = \frac{\text{TP}}{\text{TP} + \text{FN}} \tag{3.7}$$

$$\text{Averaged Sensitivity} = \frac{1}{N}\sum_{i=1}^{N}\frac{\text{TP}_i}{\text{TP}_i + \text{FN}_i} \tag{3.8}$$

Specificity is the ratio of negative instances correctly classified within all the negative instances. The averaged specificity for multiclass classification is calculated using the sum of specificity for each of the N classes.

$$\text{Specificity} = \frac{\text{TN}}{\text{TN} + \text{FP}} \tag{3.9}$$

$$\text{Averaged Specificity} = \frac{1}{N}\sum_{i=1}^{N}\frac{\text{TN}_i}{\text{TN}_i + \text{FP}_i} \tag{3.10}$$

Precision is the ratio of positive instances correctly classified within all instances classified as positive. The averaged precision for multiclass classification is calculated using the sum of precision for each of the N classes.

$$\text{Precision} = \frac{\text{TP}}{\text{TP} + \text{FP}} \tag{3.11}$$

$$\text{Averaged Precision} = \frac{1}{N}\sum_{i=1}^{N}\frac{\text{TP}_i}{\text{TP}_i + \text{FP}_i} \tag{3.12}$$

F1-score combines both precision and recall, and this metric is high only if precision and recall are both high. The averaged F1-score for multiclass classification is calculated using the averaged precision and recall of all the N classes.

$$\text{F1-score} = 2 \times \frac{\text{Precision} \times \text{Recall}}{\text{Precision} + \text{Recall}} \tag{3.13}$$

$$\text{Averaged F1-score} = 2 \times \frac{\text{Averaged Precision} \times \text{Averaged Recall}}{\text{Averaged Precision} + \text{Averaged Recall}} \tag{3.14}$$

The receiver operating characteristic (ROC) curve is another common tool the ROC curve serves as a graphical representation of the trade-off between the true positive rate (recall) and the false positive rate (ratio of negative instances correctly classified within all the negative instances). The area under the curve (AUC) serves as an evaluation metric in conjunction with the ROC curve, and the closer its value is to 1, the more TP rates the ROC curve has, and, therefore, the better the model's performance. In multiclass classification problems, the ROC curve is calculated in a one-vs-all setting where we consider one class as positive and all the others as the negative classes [83, 94, 96].

Chapter 4

Materials and Methods

In this dissertation, we aim to enhance risk assessment, both by performing an automatic and accurate posture classification and by developing a dashboard to aid ergonomists' data visualisation in the context of Autoeuropa.

This dissertation has a deep relation with the work developed in [59] and [97] leveraging its algorithms for automatic risk assessment (available in Fraunhofer's internal repository) into the developed dashboard.

The overall roadmap of the developed solution for the risk assessment illustrated in Figure 4.1, is detailed below:

1. By using the AnDy dataset [40] the goal is to perform automatic posture classification regarding more complex postures such as shoulder level and overhead work;
2. Postures feed the risk algorithms that calculate risk scores (using EAWS) and segment postures into "Acceptable" and "Not recommended" (according to ISO 11226);
3. Finally, data, risk scores and ISO segmentation are displayed in a dashboard, providing ergonomists with a user-friendly interface for enhanced data visualisation and analysis.

The present dissertation project focuses on the development of the "Automatic Posture Classification" and the "Dashboard Visualisation" steps of the entire framework presented in Figure 4.1. The development of the algorithms for EAWS and ISO 11226 implementation were provided and are not part of the developed work under this dissertation. Therefore, to tackle these topics, this dissertation is divided into two main parts, one for the posture classification task and one for the dashboard development.

4.1 Posture Classification

As previously mentioned, by using data extracted from multiple IMUs it is possible to calculate the joint angles that can be used to assess the orientation of a body segment, for example, to estimate the value of the angular flexion of the trunk. However, for more complex postures, such as overhead work, that requires information from multiple joints, the task of solely using joint angles to classify postures becomes more challenging.

With this in mind, this first section describes the usage of a CNN to perform automatic posture classification using IMU data.

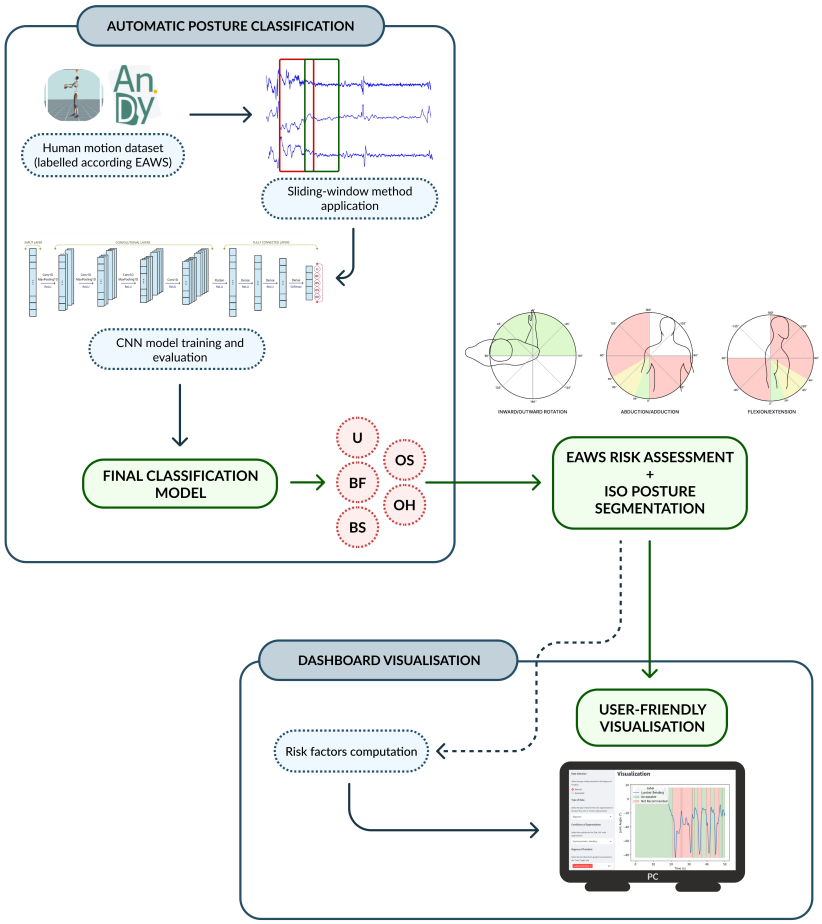

Figure 4.1: Visual representation of the entire framework for this dissertation project. The abbreviations U, BF, BS, OS, and OH correspond to the classified postures, specifically representing upright, bent forward, strongly bent forward, shoulder level work, and overhead work, respectively

4.1.1 Dataset

Within the OPERATOR project, data acquisitions were conducted at Autoeuropa to collect IMU data for training the posture classification model. However, the collected data lacked labels regarding working postures. Consequently, the AnDy dataset was employed, given its resemblance to the Autoeuropa data in terms of data characteristics, sensor types, and labelled postures. This selection ensures the seamless integration of the developed framework into data collected from workers at Autoeuropa.

The AnDy dataset comprises IMU data recorded from industry-like activities for a car manufacturing use case, labelled according to the EAWS-related postures. This choice aligns with Autoeuropa's risk assessment framework, where the workers at the automotive assembly line have their data collected through the same IMU system employed in the dataset and analysed according to the EAWS.

The AnDy dataset was developed for human motion evaluation in industrial settings and comprises thirteen participants performing several tasks totalling more than five hours of recorded data.

Firstly, the data is collected using IMUs, a marker-based optical MoCap, a contact e-glove and video recordings, being the worker's activity and posture, following the EAWS postural section (Figure C.1) annotated independently by 3 researchers.

The inertial motion system used in the dataset was the Xsens MVN Link, utilizing 17 IMUs distributed across the body by making use of a suit, as depicted in Figure B.1 in the Appendices. The suit facilitated the collection of various types of data as outlined in Table 4.1.

Table 4.1: Different types of data extracted from the 17 IMUs of the Xsens MVN Link system (according to [98]). There are 3 DoFs for each one of the 22 joint angles data.

Source	Data Types
17 IMUs	Magnetic field 3D linear acceleration Orientation (quaternion)
23 body segments of the Xsens avatar	3D position Orientation (quaternion) Linear velocity Angular velocity Linear acceleration Angular acceleration
Xsens avatar	22 joint angles (3 Dofs) Center of mass 3D position

Note that magnetic field, 3D linear acceleration and quaternion orientation data collected from the 17 IMUs are processed post-acquisition by the Xsens software, therefore, they are not raw data.

Table 4.2 presents data referent to the participant characteristics encompassing data on the number of participants, gender distribution, average age, stature, body mass, and experience level.

Table 4.2: AnDy dataset participants characteristics (from [98]).

Characteristic	Value
Number of participants	13
Gender	9 males and 4 females
Average age	25.7 ± 5 years
Average stature	175.4 ± 7.9 cm
Average body mass	72.3 ± 14.4 kg
Experience	Limited or none

The following industry-like activities performed by the participants were inspired by an automotive assembly line use case (from [98]):

- Screw high (SH): Take a screw and a bolt on a 75 cm-high table, walk to the shelf, screw at a height of 175 cm (performed with bare hands, i.e., no screwdriver).
- Screw middle (SM): Take a screw and a bolt on a 75 cm-high table, walk to the shelf, screw at a height of 115 cm.
- Screw low (SL): Take a screw and a bolt on a 75 cm high table, walk to the shelf, and screw at a height of 25 cm (6 participants) or 60 cm (7 participants).
- Untie knot (UK): Untie a knot placed on a 45 cm-high table.
- Carry 5 kg (C5): Take a 5 kg load on a 55 cm-high table, walk to the shelf, and put the load on a 20 cm-high shelf.

- Carry 10 kg (C10): Take a 10 kg load on a 55 cm-high table, walk to the shelf, and put the load on a 110 cm-high shelf.

These activities were grouped in sequences of 6 activities called trials. Each participant performed 3 different sequences 5 times, which resulted in 15 trials of 90 seconds for each participant.

From the different types of taxonomy of actions and postures used for data annotation in the dataset, the one used in this dissertation is the one related to "detailed postures". These are related to the EAWS section of trunk and arms postures and movements presented in Figure 3.6. The dataset's considered "detailed postures" are presented in Table 4.3.

Table 4.3: "Detailed postures" used for data annotation according to EAWS's "Basic Positions/Postures and movements of trunk and arms (per shift)" section from [98].

Label	State	Description
U	Upright	Torso straight
BF	Bent forward	Torso flexion angle between 20°and 60°
BS	Strongly bent forward	Torso flexion angle greater than 60°
OS	Shoulder level work	Elbow(s) at or above shoulder level with hand(s) at or below head level.
OH	Overhead work	Hand(s) above head level.

4.1.2 Preprocessing

Before proceeding with the ML methods for posture classification, data needs to be preprocessed.

The objective is to undertake posture classification, focusing on more intricate postures such as shoulder level and overhead work postures. The initial step involved the extraction of relevant data for the task from the comprehensive dataset available in the AnDy dataset. The Xsens MVN Link collects many types of data as presented in Table 4.1. For this dissertation project, we focused on data from the upper body and performed a pre-selection of data types to use. This information is summarized in Table 4.4.

Table 4.4: Selected types of data, joints and sensor positions for this dissertation.

Data Types	Joints	Sensor Positions
Joint Angle	L5-S1	T8
Acceleration	Right and Left Shoulder	Right and Left Upper Arm
Angular Acceleration	Right and Left Elbow	Right and Left Forearm
	Right and Left Wrist	Right and Left Hand

The second step was to compute the magnitude vector of the x, y and z components of position, velocity, acceleration, angular velocity, angular acceleration, sensor-free acceleration and sensor magnetic field according to Equation 4.1.

$$|magnitude| = \sqrt{x^2 + y^2 + z^2} \tag{4.1}$$

The next step was to use interpolation to match the IMU data and the annotations, since the IMU data was collected at 240 Hz, while the video recordings for the annotations were recorded at 25 fps.

After this, the data was downsampled from 240 Hz to 60 Hz, which was achieved by selecting data instances from the original data at a time step of 0.01667 s ($\frac{1}{60}$) and allowed the model to be trained faster as data between the selected time points was removed. The last preprocessing step was window creation using the sliding window method. The windows were created using 200 data points, and an

overlap between windows of 0.25. This means that each window had approximately 3.33 seconds and included the last 25% of data points from the previous window. This method is exemplified in Figure 4.2

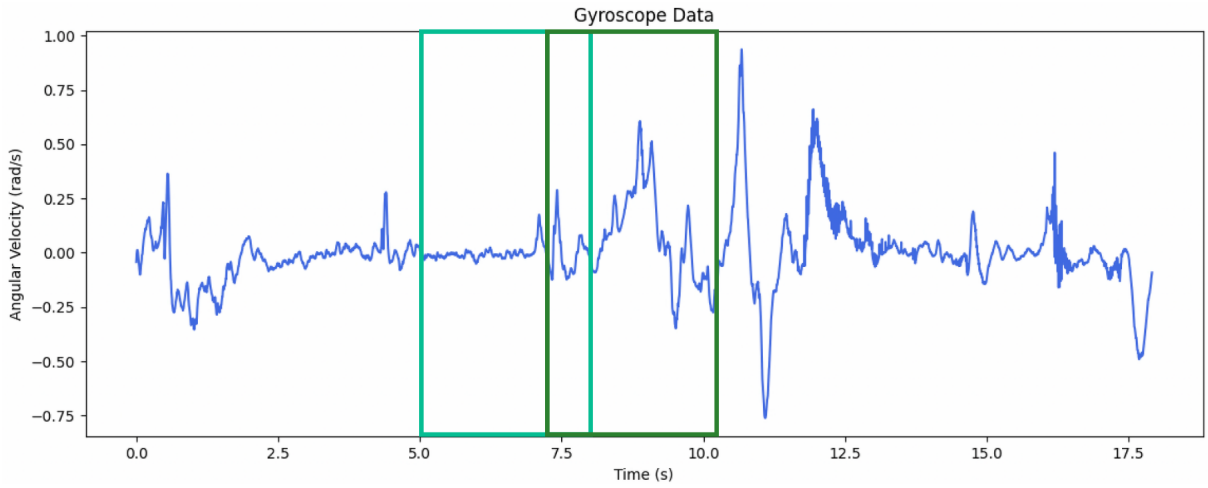

Figure 4.2: Sliding window representation on gyroscope data.

One final remark regarding the dataset is that the considered postures are not equally present, making the dataset unbalanced. Considering the total number of windows created, U postures accounted for 66% of the data, BF for 10.9% of the data, BS for 14.4%, OS for 2.9% and OH for 5.8%, approximately.

4.1.3 Machine Learning

The posture classification algorithms were developed using Python 3.8, and TensorFlow 2.12. High-performance computing was also utilized for model training, with several GPUs being available: two 1xV100 16G, one 2x V100 32G and one 1xV100S 32G.

4.1.3.1 Feature Extraction

An ML model uses features to perform classification on time series. These features represent characteristics of the data that preserve the core information while reducing its dimension. Several features can be extracted from each window considering data time series such as the data that comes from IMUs evidenced in Figure 3.7.

The Time Series Feature Extraction Library (TSFEL) is a feature extraction tool for time series that automatically extracts up to 60 different features on the statistical, temporal and spectral domains [99].

In this dissertation, the available statistical features were computed for the different data types (evidenced in Figure 4.1). Besides these calculations were performed for each data window, being then used as the inputs of the ML models tested. The used TSFEL statistical features have linear complexity and are presented in Table 4.5.

4.1.3.2 Data Splitting

As previously stated in Section 3.4.3 data split is an important step in ML validation and is important that it ensures two aspects to avoid biased conclusions. The first is that the classes need to be balanced between both datasets, this means that the labels used for classification are equally represented in the training and test datasets. The second is that a subject's data is not present in both datasets, this means that if the training set has data from a subject, the same subject will not have any data in the test dataset.

Table 4.5: TSFEL statistical domain features [99].

Features
Absolute energy
Average power
ECDF
ECDF Percentile
ECDF Percentile Count
Entropy
Histogram
Interquartile range
Kurtosis
Max
Mean
Mean absolute deviation
Median
Median absolute deviation
Min
Root mean square
Skewness
Standard deviation
Variance

Unable to split the data in a way that ensured both subject split and data balance between the training and testing datasets we opted for a cross-validation approach namely the leave-one-subject-out cross-validation (LOSOCV). This cross-validation method is similar to the k-fold cross-validation method explained in Section 3.4.3, but instead of each one of the k-folds being used as the test dataset iteratively, the data from a single subject is used as the test dataset while all the other subjects are part of the training dataset (as represented in Figure 4.3) [100, 101].

Figure 4.3: Leave-one-subject-out cross-validation method, each subject is used as the test set once (adapted from [101]..

4.1.3.3 Hyperparameter Tuning

To facilitate model hyperparameter tuning, a validation set was introduced within each fold of the (LOSOCV). This process resulted in the establishment of two sequential LOSOCVs. In the initial cross-validation step, one subject's data was designated as the test set out of the 13 subjects in the dataset.

Among the remaining 12 subjects, one was randomly chosen as the validation set, while the other 11 formed the training set. In this phase, the second cross-validation took place for hyperparameter tuning. Consequently, for each subject chosen as the test dataset, the remaining 12 subjects underwent a LOSOCV, where each subject's data was iteratively used as the validation set to assess the best hyperparameter combination. This combination was then used to train the entire twelve subjects and then tested on the previously selected test subject.

The posture classification task was performed by four different classifiers: DT, RF, SVM, GNB. Table 4.6 presents the tested hyperparameters and their values, as well as the optimised values obtained for each model. The hyperparameter optimisation step was executed using Grid Search. Additionally, the optimised values were determined based on the best hyperparameter combination from each of the 13 tested folds, selecting the values associated with the fold that exhibited the highest accuracy score.

Table 4.6: Hyperparameters tested, the respective values and the optimised values, for each classifier.

Classifier	Hyperparameters	Tested Values	Optimized Value
DT	max_depth	None, 10	10
	min_samples_leaf	1, 5	1
RF	n_estimators	10, 50	50
	max_depth	None, 10	None
SVM	C	0.1, 10, 100	0.1
	penalty	l1, l2	l2
GNB	var_smoothing	1 to 10^{-9} (10 iterations)	0.1

Finally, the multiclass confusion matrix was computed along with the evaluation metrics.

4.1.4 Deep Learning

The data used for the deep learning method followed the same preprocessing as the ML approach as described in Subsection 4.1.2.

Moreover, instead of using features extracted from each window, the data types from the AnDy dataset were used directly. However, this data required prior normalisation and so, according to Equation 4.2, the data was normalised for each window.

$$\text{Normalized Data} = \frac{\text{Data} - \text{Mean}}{\text{Standard Deviation}} \tag{4.2}$$

Once again, the LOSOCV approach was used, but without any validation set. Instead, each of the 13 subjects was used as the test set once in each fold, while the other 12 subjects were in the training set.

4.1.4.1 Model

The developed model for the classification task was a simple CNN with an input layer, followed by convolutional layers. The feature extraction section of the network is composed of three 1D convolutional layers alternated with max-pooling layers, and another 1D convolutional layer at the end. Each 1D convolution possesses twice the number of filters of the previous one. Finally, the classification section of the network is formed by one flattened layer and three dense layers. The ReLU activation function is used throughout the whole network except for the last dense layer where the softmax activation function is used to compute the probability of a data window belonging to each one of the five classes.

Figure 4.4 illustrates the CNN architecture.

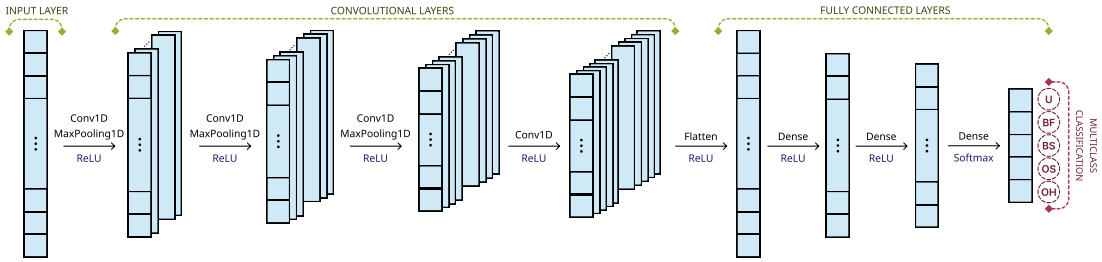

Figure 4.4: Illustration of the used CNN architecture.

The model's input is a matrix of shape (window size, IMU signals), and here IMU signals refer to the raw signal from the IMUs and derived joint angles. Initially, the window size was set to 200 points, while 36 IMU signals were chosen, totalling 10110 data windows. Regarding the convolutional layers, the number of filters was set to 32 and the filter size was defined as 7. The Adam optimiser was selected with an associated learning rate of 0.0001, and the loss function considered for this problem was the categorical cross-entropy. Furthermore, the number of epochs was set to 100 and the batch size was 32. This implies that the entire dataset undergoes training 100 times, with 32 training instances processed in each iteration.

One used parameter was class weights since these are specially used to handle imbalanced datasets. These datasets have some classes with significantly fewer samples than others. Moreover, class weights enhance the importance the model gives to the less represented classes, downplaying the importance of the most represented ones.

Equation 4.3 presents the method for calculating each class weight according to scikit-learn [102]. In this equation, the weight for a specific class is the total number of samples of every class (TNS) divided by the number of existent classes (NC) multiplied by the number of samples that class has (NSC).

$$\text{Class Weight}_i = \frac{\text{TNS}}{\text{NC} \times \text{NSC}_i} \tag{4.3}$$

Several model hyperparameters were tested and optimised for a better classification. Table 4.7 shows the optimised hyperparameters.

Table 4.7: Hyperparameters tested, the respective values and the optimised result for the CNN.

Hyperparameter	Tested Values	Optimized Value
Number of Filters	16, 32	16
Kernel Size	3, 7, 10	7
Batch Size	16, 32, 64	32
Learning Rate	0.00001, 0.00005, 0.0001, 0.001	0.00001

The window size was also changed from the initial 200 instances (roughly corresponding to 3.33s) selected based on [32] that stated that for activity recognition on the upper body, a window size of 1 to 4.5 s allows for the best recognition performance. In [39] a window size of 250 ms with an overlap of 50% was used. With this in mind, window sizes of values of 30 and 15 instances were tested, corresponding to, 500 ms and 250 ms of data, respectively.

Finally, the predicted labels for both shoulder level (OS) and overhead work (OH) were saved and integrated into the risk algorithms to make up for the inability to detect these postures solely relying on angular data.

4.2 Dashboard

4.2.1 User Perspective

The dashboard allows precise data visualisation for the ergonomics practice. Unstructured interviews were conducted with two Autoeuropa's ergonomists.

These interviews served the purpose of defining the technology requirements for the dashboard development and were based on the ergonomists' difficulties as well as the risk indicators they look for when performing risk assessment.

4.2.2 Components/Sections Development

The dashboard was specifically developed for Autoeuropa's ergonomics team use case, using Streamlit and Python. As previously explained, the dashboard takes the data from the risk algorithms to build visualisations. Postures feed the risk algorithms, which, in turn, calculate risk scores utilizing the EAWS and segment postures into "Acceptable" and "Not recommended" categories following the criteria outlined in ISO 11226. These algorithms were based on a risk assessment guideline sheet as presented in Figures C.1 and C.2 in the Annexes adapted from [97].

The guidelines use an adapted version of EAWS' "Basic Positions / Postures and movements of trunk and arms (per shift)" focused on the "Standing (and Walking)" section. It is important to highlight that, for extreme postures, the criteria chosen was the one outlined in EAWS, as opposed to the criteria defined in ISO standard 11226, since EAWS incorporates a broader spectrum of values to define extreme postures, increasing the biomechanical exposure to risk factors.

Within the scope of this dissertation, the guidelines suffered some modifications, namely on the ranges of conditions for the trunk and upper arm postures, to enhance the dashboard's comprehension and displayed information. Further implementations were performed to present more information than the one that came from the risk algorithms. To complement the developed graphical visualisations, some metrics were computed that allow for further insight into the presence of awkward posture and task repetitiveness, in terms of exposure duration and occurrences, respectively. The duration of exposure is given by the sum of every period under the same posture or condition. For example, the total duration a worker is under a risky posture regarding upper arm elevation is given by the sum of every period the worker is in a not recommended upper arm elevation posture. The repetition of exposure is given by the number of times a risk period occurs independently of its duration.

Figure 4.5 presents how the duration and repetition are assessed in the dashboard. The presented segmentation is given by the intensity of postures provided by the standard guidelines ISO and EAWS. The duration is assessed through the exposure to risk postures. This metric was calculated as a percentage of the selected work cycle window. This risk exposure metric indicates the percentage of worked time the worker spent on an "Acceptable" or "Not Recommended" working posture, or on a certain angular condition, according to ISO. Additionally, the repetition was assessed through the number of risk posture occurrences. This metric represents the number of times a worker went to an "Acceptable" or "Not Recommended" working posture, or repetition of a certain angular condition (for example the number of instances a worker was in a strongly not symmetric trunk rotation posture), according to ISO.

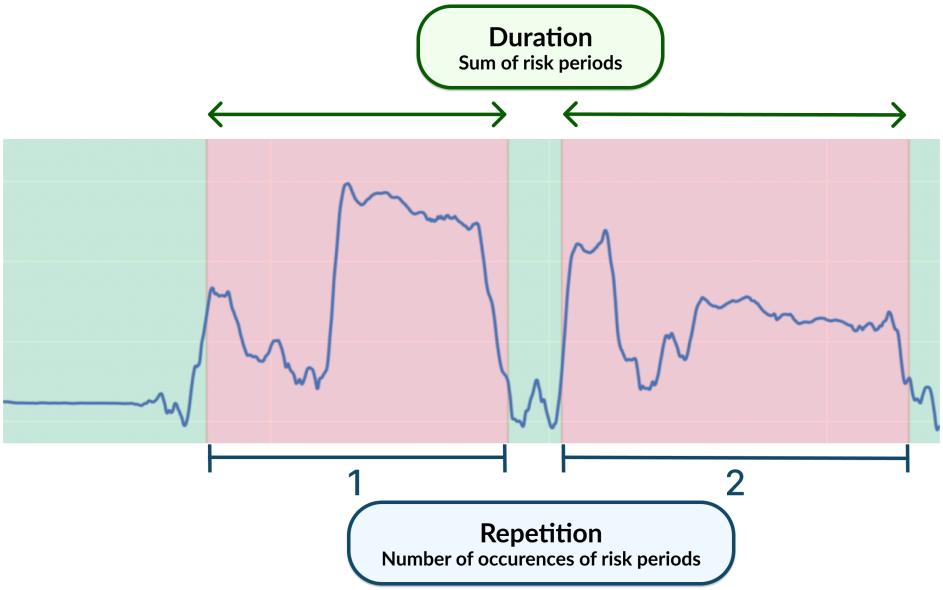

Figure 4.5: Duration and repetition assessment of angular data.

Chapter 5

Results and Discussion

5.1 Posture Classification

In this section, we present the outcomes of the posture classification task outlined in 4.1. The postures under consideration include standing upright (U), bent forward (BF), strongly bent forward (BS), shoulder level work (OS), and overhead work (OH). It's noteworthy that these positions align with the "Basic Positions/Postures and movements of trunk and arms (per shift)" section of EAWS, visually depicted in Figure C.1.

The primary focus of classification targets OS and OH. For the remaining postures, such as standing upright and bent forward, accurate classification can be easily and precisely achieved through straightforward definitions of angular limits derived from the joint angle data obtained from the IMU signal. Consequently, the application of a complex model like a CNN is deemed unnecessary for these specific classifications.

Conversely, OS and OH postures present greater complexity, requiring information from multiple joint angles for their definition. Detecting these postures poses a more intricate challenge compared to the previously mentioned ones. Consequently, sophisticated methods were developed to assess OS and OH postures, initially employing machine learning solutions i.e., using four distinct classifiers and then applying a deep learning model, i.e. CNN, as described in Sections 4.1.2 and 4.1.3, respectively.

5.1.1 Machine Learning

In the initial strategy for posture classification, the data of the five targeted postures underwent segmentation into windows encompassing raw data for acceleration, angular acceleration, and the derived joint angles. To carry out posture classification, four distinct classifiers were employed, and the corresponding outcomes are outlined in Table 5.1.

Table 5.1: Accuracy, precision, recall and F1-scores for each classifier. The presented precision, recall and F1-scores correspond to the OS and OH postures, while the accuracy refers to the average accuracy for the entire classification

Classifier	**Accuracy**	**Precision**		**Recall**		**F1-Score**	
		OS	OH	OS	OH	OS	OH
DT	0.84	0.51	0.68	0.27	0.85	0.35	0.76
RF	0.88	0.62	0.72	0.29	0.87	0.39	0.79
SVM	0.86	0.41	0.71	0.33	0.72	0.37	0.72
GNB	0.68	0.00	0.23	0.00	0.16	0.00	0.19

Table 5.1 presents the average accuracy in the context of the LOSOCV approach for the classification

task. The RF exhibited the highest accuracy with a score of 0.88. Nevertheless, relying solely on accuracy as an evaluation metric may not be sufficient for addressing the complexities inherent in the classification of working postures, particularly emphasizing OS and OH. Given the multi-classification nature of the problem, misclassifying a sample from a rare class may carry more significance than misclassifying a sample from a more frequent class, which is not accounted for by the accuracy metric. Additionally, the existence of imbalanced datasets introduces potential bias, as a model might appear to achieve high accuracy by predominantly predicting the most prevalent class.

Recognizing these limitations, the F1-score emerges as a much more adequate metric for model evaluation. By combining precision and recall, the F1-score provides a more comprehensive assessment. For instance, a high F1-score for OS postures signifies the model's accurate identification of OS data while not misclassifying other classes as OS. When examining the F1-score for OS and OH postures, the RF classifier produces the best results for both postures. However, it is noteworthy that the achieved result for the OS posture is notably low with an F1-score of 0.39.

For a more comprehensive understanding of the classifier's performance in each posture classification, we can analyze the CM related to RF classifier's results, as illustrated in Figure 5.1. This figure illustrates the predicted classes versus the true classes generated by the classifier. Regarding the most relevant classes for this dissertation specific postures, the CM highlights the model's suboptimal performance in precisely classifying the OS posture. Specifically, the majority of OS postures are misclassified as OH.

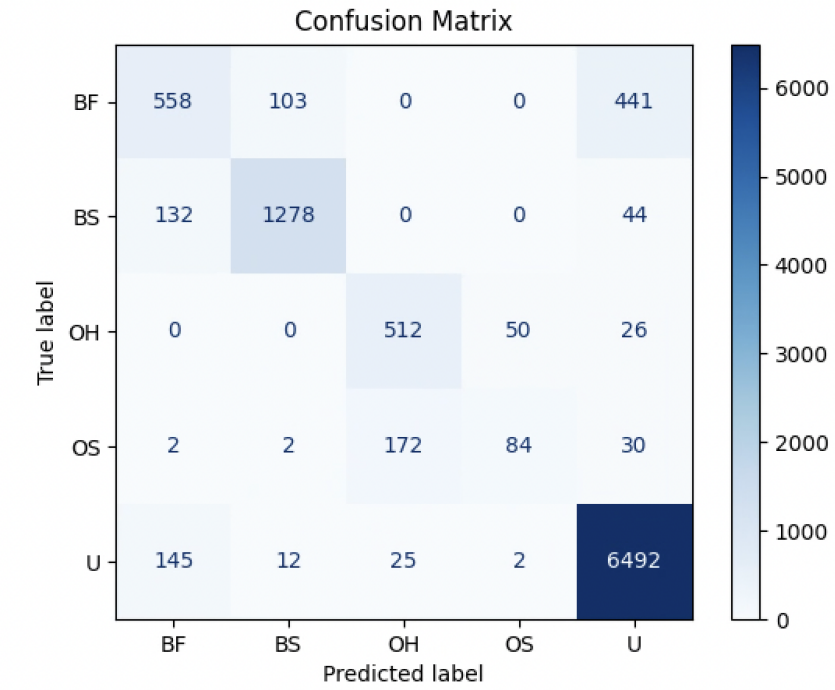

Figure 5.1: Random forest classifier confusion matrix.

The study of [36] performed the classification of correct and incorrect postures during lifting and releasing weights. This study used the SVM and tested 3 different weights. The mean recall values achieved for the 3 weights were 0.979 and 0.991 for lifting and releasing the weight, respectively.

Additionally, the study of [37] used one accelerometer data to classify both static postures and activities. This study used RF and SVM classifiers and the lowest individual F1-scores achieved were 0.92 and 0.90, respectively.

The authors of [36] and [37] reported high recall and F1-score values for various posture and activity classification tasks using IMUs. However, the results achieved for OS and OH work classification exhibited suboptimal performance. Based on these preliminar results, as presented in Table 5.1 and Figure 5.1, it can be concluded that distinguishing between OS and OH working postures poses a challenge for traditional ML classifiers.

In response to this limitation, a DL approach was considered to enhance the classification results in comparison to traditional ML classifiers. Subsequently, a CNN model was developed.

5.1.2 Deep Learning

The development of the CNN adhered to the processes outlined in Sections 4.1.2 and 4.1.4.

Hyperparameter testing for the model followed the sequence detailed in Table 4.7. The initial configuration involved 32 filters, a kernel size of 7, a batch size of 32, and a learning rate of 0.0001. Subsequently, the evaluation proceeded with an assessment of the number of filters, followed by the filter size, batch size, and ultimately, the learning rate. For each hyperparameter, values were tested, and the one that demonstrated improved results was selected as the optimized value. The optimized values for these hyperparameters are visually depicted in Table 4.7. Additionally, the window size and overlap were altered to discern their impact on the model's performance. Firstly, a window size of 200 time instances (3.33 s) was used with a 25% overlap. Then, a window size of 30 instances (0.50 s) with 25% overlap was tested, followed by a window size of 15 instances (0.25 s) with 50% overlap.

In the context of selecting the best model, reliance solely on the accuracy metric is inadequate due to the unbalanced class distribution in the dataset.

In alignment with the evaluation of classifiers, the F1-score initially emerged as a primary metric for model assessment. However, in the specific context of OS and OH posture classification, recall demonstrated itself as a more precise metric for evaluating model performance. Ensuring a high recall holds particular significance in scenarios where missing a positive instance is more consequential than having false positives in other words, accurate classification of OS and OH postures is crucial due to their elevated risk levels, as indicated by the highest associated risk per unit time according to the EAWS. Correct identification of these postures is pivotal for facilitating ergonomic interventions.

A high recall value signifies the model's proficiency in capturing all instances of a specific posture. For example, a high recall for OS indicates the model's effectiveness in identifying working postures with arms at shoulder level. Conversely, high specificity indicates the model's proficiency in identifying working postures with arms not at shoulder level. Therefore, a high recall is preferred as the correct identification of these postures is crucial for supporting conservative/protective ergonomic interventions.

Following these considerations, the model that presented the highest OS and OH recall scores has the hyperparameter values and window configuration presented in Table 5.2.

The utilization of a CM provides valuable insights into the behaviour of the model concerning the posture classification task. The CM of the best model's results is depicted in Figure 5.2. Note that using a smaller window size of 0.5 seconds resulted in more windows to classify when compared to the window size of 3.33 seconds used in the ML classifiers and the first evaluated DL models. The window size of 0.5 s resulted in 68934 windows while the 3.33 s window size resulted in 10110 windows of data.

By analysing the CM we can perceive that the model as a general rule distinguishes with high precision the different classes. Regarding OS and OH postures, the focus postures of this thesis, it becomes evident that a notable portion of misclassifications for these classes occur when the model confuses the OS class for OH and vice versa. This outcome aligns with expectations, given the substantial similarity

Table 5.2: The proposed model parameters and their values. Parameters refer to the model's hyperparameters and the window configuration parameters.

Parameters	Value
Batch Size	32
Epoch	100
Learning Rate	0.00001
Kernel Size	7
Number of Filters	16
Window size	30 (0.50 s)
Overlap	25%

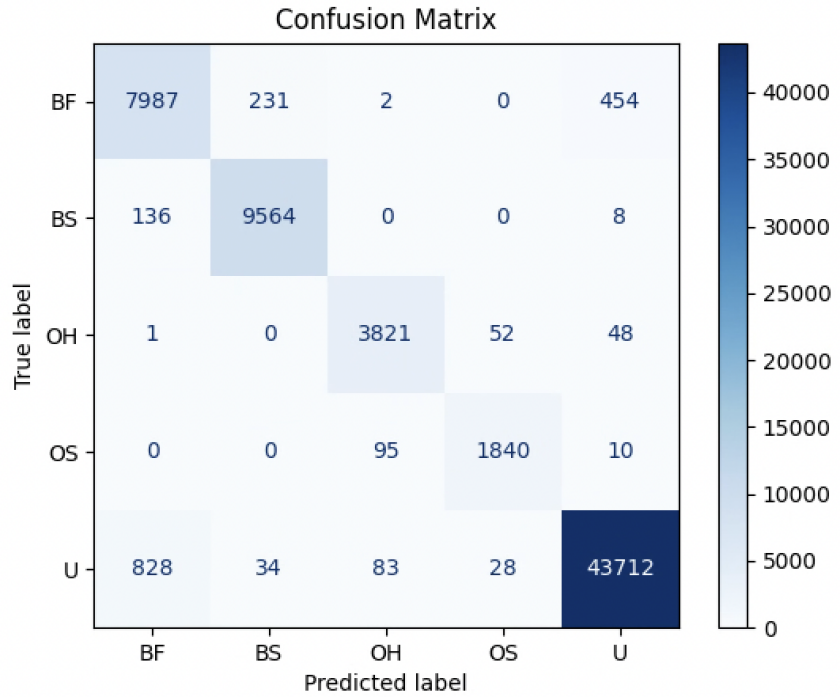

Figure 5.2: Confusion matrix for the proposed model.

between shoulder level and overhead work postures. Moreover, instances arise where the model classifies OS and OH postures as U. This phenomenon may be attributed to the prevalence of the U posture, the most common one in the dataset. A similar occurrence is observed for the BF posture, which often receives classifications as U, and vice versa.

Table 5.3 shows an example of a classification report presenting data on the precision, recall and F1-score for the proposed model. The support value presented in the table refers to the number of windows for each class and in total.

Moreover, despite the relatively low occurrence of OS and OH postures, comprising only 1945 and 3922 windows, respectively, out of a total of 68934 windows, our model achieved commendable recall scores of 0.95 for OS and 0.97 for OH. These scores affirm the model's capability to accurately identify instances where a worker assumes postures with arms at shoulder level or above the head.

Furthermore, the high F1-scores of 0.95 for OS and 0.96 for OH also indicate the model's proficiency in accurately identifying these postures amidst other classes, without misclassifying other postures as OS and OH.

It is noteworthy that the chosen model does not boast the highest overall accuracy value, nor the best macro average value for the recall or F1-score. Instead, it is selected based on its achievement of the

Table 5.3: Classification report for the proposed model

Classification Report

Class	Precision	Recall	F1-score	Support
BF	0.89	0.92	0.91	8674
BS	0.97	0.99	0.98	9708
OH	0.96	0.97	0.96	3922
OS	0.96	0.95	0.95	1945
U	0.99	0.98	0.98	44685
Macro Average	0.95	0.96	0.96	68934
Weighted Average	0.97	0.97	0.97	
Accuracy		0.97		

highest recall specifically for the most crucial postures within our problem context, namely the OS and OH working postures.

The effectiveness of LSTM networks for activity recognition in ADL has been demonstrated by the authors of [33], [34], and [35]. Furthermore, in [38], an LSTM-based network was employed for posture classification in seated positions, achieving an average F1-score of 0.966.

In a related study, the authors of [35] utilized an LSTM network to achieve an F1-score of 0.958 in activity classification on the Skoda dataset, an automotive industry-like dataset. Despite the LSTM model outperforming a CNN model (0.893) in the activity recognition task, questions persisted regarding how the CNN model would perform in a posture classification problem where the temporal aspect of the data is less relevant.

Using the outlined CNN model, the average F1-score achieved across each classified class, represented as the macro average, stands at 0.96. Table 5.4 presents the number of features and F1-score achieved by the authors of [39] and by the CNN proposed in this dissertation. Using the final selected subset of features the authors in [39] achieved an F1-score 0.94. Additionally, the highest F1-score was achieved when using all data relative to segment positions as features, comprising 69 features and an F1-score of 0.96. It's worth noting that the suggested CNN attains an identical F1-score of 0.96 with a reduced subset of 35 features. The utilization of smaller feature subsets contributes to an enhancement in model training efficiency.

Table 5.4: Number of features and F1-score for the model proposed by the authors of [39] and the developed CNN.

Model	**Number of Features**	**F1-score**
[39]	6	0.94
	69	0.96
Proposed CNN	35	0.96

Figure 5.3 presents the loss and accuracy plots for the best model. The loss plot indicates a rapid initial decline in loss during the early stages of training, followed by a more gradual decrease in subsequent iterations. Similarly, the accuracy plot exhibits a swift rise in accuracy during the initial training epochs, followed by a slower increment in subsequent epochs. Consequently, the number of epochs is sufficient for the model to converge, as the loss values suffer little to no change for higher epochs, suggesting the potential use of fewer epochs in the training process. Moreover, the implementation of an early stopping method could have been considered to stop the training process at an earlier stage.

Other noteworthy considerations include the observation that only four out of the total thirteen sub-

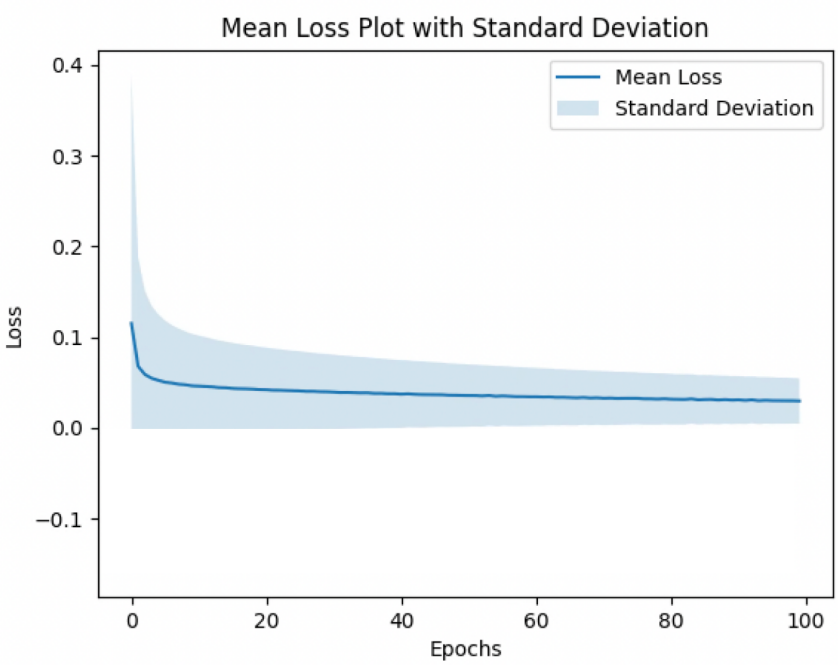

(a)

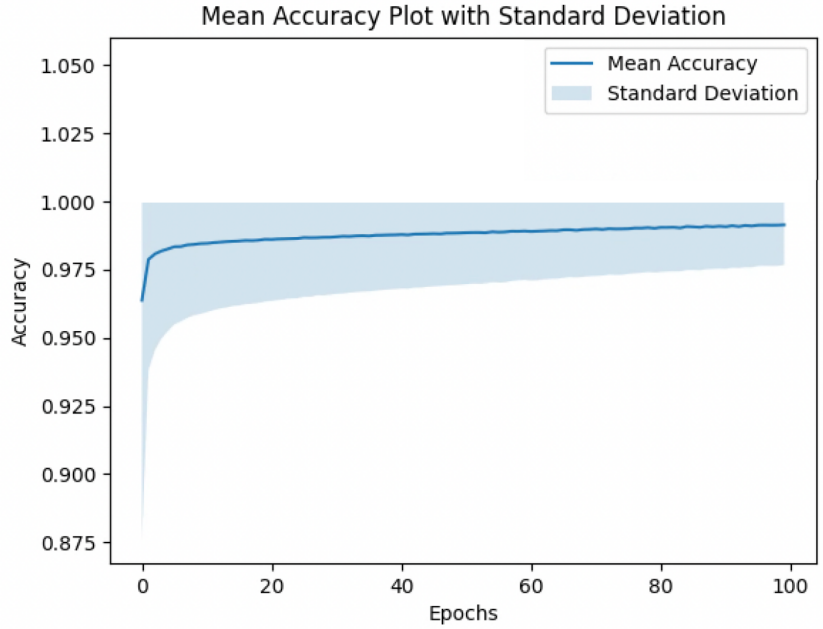

(b)

Figure 5.3: (a) presents the loss plots with the respective standard deviation. (b) shows the accuracy plot and the respective standard deviation for the proposed model.

jects possess all five labels. Furthermore, among the thirteen subjects, seven subjects included data featuring the OS posture, while ten subjects incorporate the OH posture in their data. This situation posed challenges in data splitting, requiring a balance between class stratification and subject data separation for training and test sets. Consequently, a cross-validation approach, though computationally demanding, was employed. The ML approach faced challenges due to the computational burden of the two consecutive LOSOCV processes required for model evaluation and hyperparameter tuning. The feature extraction process required by ML classifiers also added to the computational burden of this approach.

These limitations imposed constraints on testing parameters without compromising the classifier's training time.

Moreover, the dataset's imbalance, with the two relevant postures (OS and OH) being underrepresented, hindered classification efficiency. The scarcity of true positive instances for these classes further impacted the classification performance. To address this issue, class weights were incorporated as a mitigating measure.

An additional limitation was the use of only one set of data types for the CNN development, incorporating acceleration, angular acceleration, and joint angle data for the classification task. However, the decision was made not to explore different data types, as the model demonstrated high performance with the selected data.

5.2 Dashboard

5.2.1 Requirements to Features

Table 5.5 presents the ergonomists' difficulties and needs that were expressed during the unstructured interview and the dashboard's adaptation to such requirements.

The demand for automating the laborious and time-consuming EAWS filling process gave rise to the development of feature I1.

The ergonomists expressed the lack of visual support for ergonomics analysis, prompting the creation of feature V1. This, combined with the necessity to detect periods of worker exposure to risk postures, resulted in the development of features V2, V3, and V6, incorporating visualizations with segmented data.

Two critical factors in evaluating work are the duration and repetitiveness of exposure to risk postures. These aspects are addressed through the coloured segmentation of features V4 and V5, along with metrics for duration and repetition in features I3 and I4.

Additionally, feature I2 was developed following the need to analyse different body segments separately, e.g., the right and left upper arms independently. Furthermore, addressing the challenge of identifying the optimal work cycle sequence for a specific worker is the focus of feature I5. Finally, the need for interactive analysis of risk exposure over time led to the development of feature I6, allowing navigation through the time window.

Ergonomists dedicate their efforts to enhancing work processes, aiming to optimize production sustainably while ensuring workers' safety and well-being. In pursuit of this objective, ergonomists consider various factors when conducting risk assessments. Ideally, they aspire to devise an optimal sequence of workstations that minimizes each worker's risk of developing WRMSDs, taking into account individual needs. Key factors in this process include:

- Each workstation's relative risk as certain workstations may expose workers to risky postures more frequently than others;
- The sequence in which the workers navigate through workstations. Ideally, more challenging workstations may be strategically placed and spaced throughout the shift;
- The specific constraints of each worker and their association with different workflows. This personalization aims to maximize productivity while considering factors such as a worker's experience or injuries. For example, a worker's experience is a factor in the worker's exposure to risk

posture and MSDs. Moreover, adapting tasks for workers with injuries or health conditions can not only maintain productivity but also expedite recovery. For instance, assigning tasks with reduced impact to a worker with an injured right shoulder can prevent downtime while supporting recuperation. This way, sending workers home can be avoided while maintaining productivity.

Table 5.5: Ergonomists' difficulties and needs when performing risk assessment in Autoeuropa, expressed during an unstructured interview. Also presented are the requirements for each difficulty/need and the correspondent dashboard feature developed, along with a code for easy identification. The features related to the created visualisations are identified with a "V", while the ones related to data and the interaction of the ergonomist are identified with an "I".

Ergonomist Difficulty/Need	**Requirement**	**Dashboard Feature**	**Code**
Laborious and time-consuming filling of the EAWS	Filling the EAWS worksheet	Automatic calculation of the percentage of exposure and risk scores associated with each of the EAWS "Standing (and walking)" postures	I1
Visually identifying extreme postures for a body segment	Information about the different DoFs' angles over time	Graphical presentation of the angle vs time for the DoFs of each body segment	V1
	Precise categorization under angular constraints	Graphical presentation of angular segmentations using adapted ISO norm angle categories	V2
	Precise categorization under angular constraints	Graphical presentation of posture-related risk segmentation according to ISO ("Acceptable" and "Not recommended" postures)	V3
Assess the risk and exposure of different body parts separately	Separate analysis for each body segment	Allows to choose between each body segment for risk exposure analysis	I2
Detection of prolonged risk exposure during work	Visual display with easy identification of a worker's exposure to risk postures	Graph with colour segmentation allows easy detection of **longer periods** with risky postures	V4
Assessment of work repetitiveness	Visual display with easy identification of a worker's exposure to risk postures	Graph with colour segmentation allows easy detection of **several instances** of a risky postures	V5
	Calculation of a metric for risk posture exposure in terms of repetition	Calculates the number of occurrences of exposure to a "Not Recommended" ISO position for each DoF of each body segment	I3
Identifying which tasks hinder greater risk to a worker's hurt body segment recuperation (i.e., segment with a musculoskeletal lesion)	Identification of periods a body segment is greatly exposed to risk	Calculates the exposure to a "Not Recommended" ISO position for each DoF of each body segment, in percentage of the work cycle	I4
		Graphically presents a larger red zone identifying the moment in the work cycle when an extended period of risk exposure happened	V6
Identifying which task rotation is better for a worker under recuperation	Calculate a metric capable of comparing different rotation tasks	EAWS risk scores are calculated for the entire work cycle or for the entire shift (sequence of work cycles)	I5
Analyze risk exposure over time	Navigate through the time window	Slider that allows time windows visualization and navigation	I6

5.2.2 Features Development

A comprehensive overview of the dashboard is provided in Figure D.1 in the Annexes. This section will highlight the primary features and visualisations generated by the dashboard. The data showcased in the dashboard originates from a single trial of the AnDy dataset.

Commencing with the data selection window, as illustrated in Figure 5.4, this section is pivotal for selecting the data utilized in the dashboard's visualisations and tables.

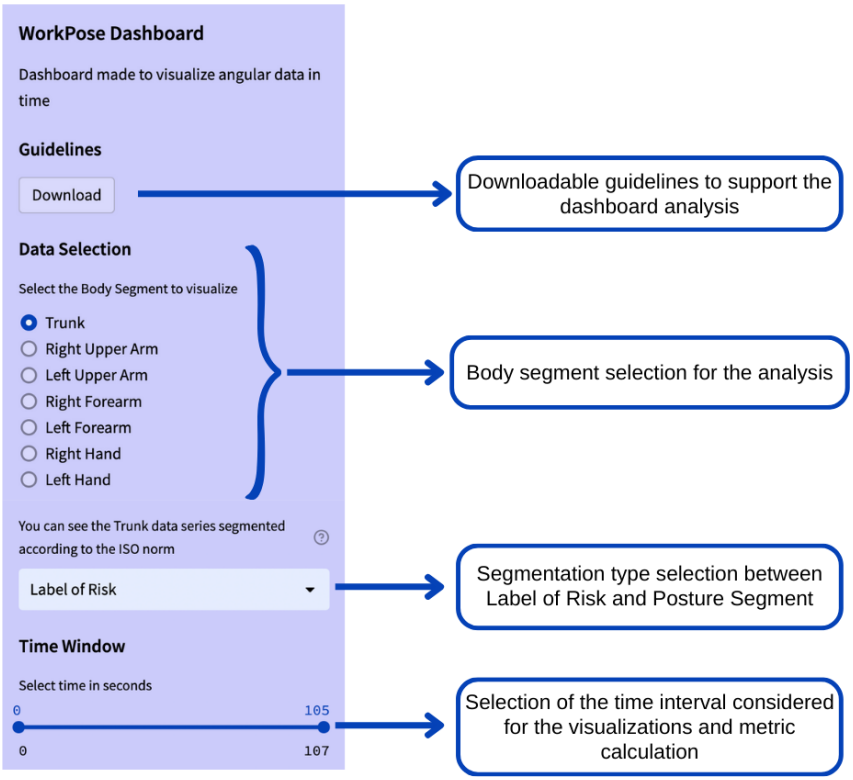

Figure 5.4: Dashboard window that allows data selection and respective description.

Initially, guidelines presented in Figures C.1 and C.2 can be downloaded to aid in interpreting and analyzing the dashboard. Subsequently, the "Data Selection" section enables users to select the upper body segment for assessment, allowing separate evaluation of the left and right segments of the upper arms, forearms, and hands. Within this section, users can also choose the type of segmentation applied to the time series following ISO norm 11226. The "Label of Risk" segmentation categorizes data into "Acceptable" and "Not Recommended" sections, while the "Posture Segment" divides the data based on angle limits for the selected body segment. The time window slider defines the considered time period for the dashboard, facilitating navigation through visualisations and serving as a reference for calculating metrics. The "Data Selection" window can be hidden to optimize data visualisation.

Moving on to the dashboard visualisation section, as depicted in Figure 5.5, this segment provides visual support for ergonomic risk assessment.

Initially, the visualisations encompass the complete time series data for the chosen body segment, along with the respective DoF data plotted.

Next, the figure displays trunk/lumbar rotation, followed by lateral bending and lumbar flexion/extension. These plots illustrate the angles of DoF over time, with the data segmented according to ISO norm 11226 into "Acceptable" and "Not Recommended", represented by green and red colors, respectively. Therefore, corresponding to "Label of Risk" visualisation.

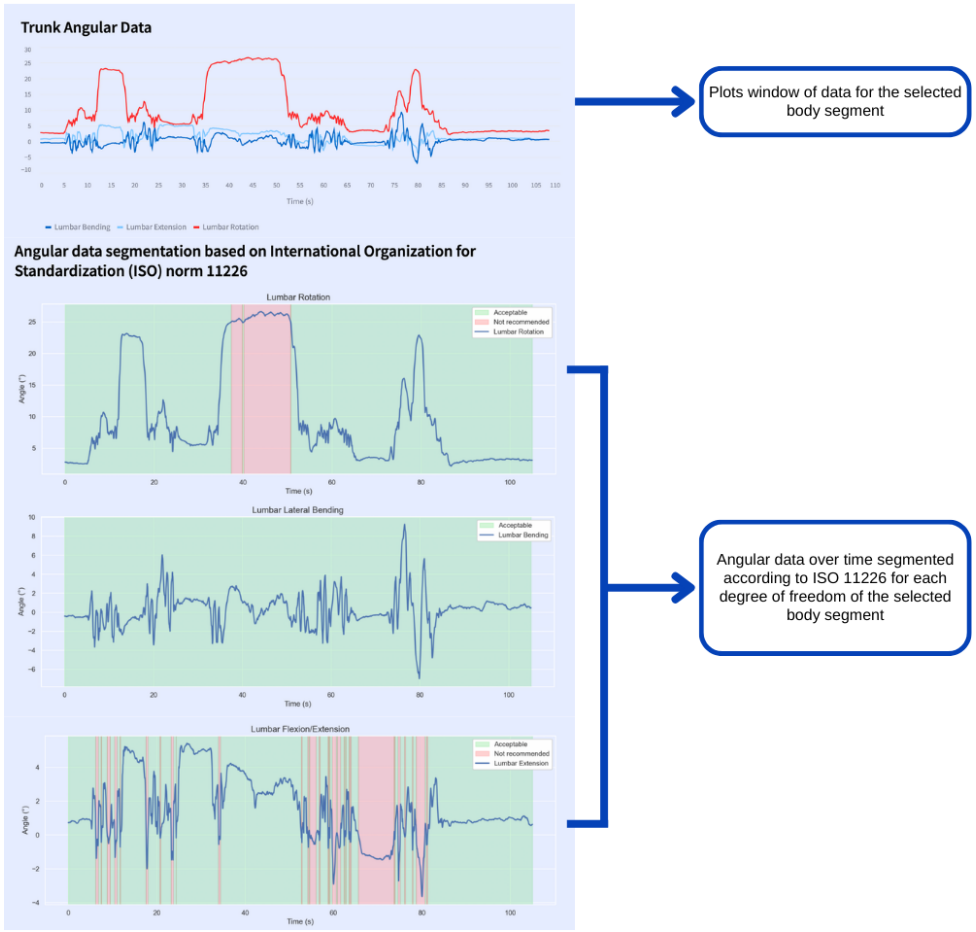

Figure 5.5: Dashboard's section for data visualisation and respective description. The data refers to the trunk and the segmentation presented is based on ISO 11226 ("Label of Risk").

Moreover, Figure 5.6 also features another visualisation section of the dashboard. The distinction lies in the selected segmentation type in the "Data Selection" window of the dashboard. The graphs presented using the "Posture Segment" segmentation offer a more detailed segmentation considering angular data, delineating divisions based on several angular limits. This segmentation aligns with the angular limits previously introduced in Figure C.2.

Subsequently, within the metric section, the dashboard provides metrics derived from the visual representations aforementioned.

Figure 5.7 showcases metrics corresponding to the segmentation depicted in Figure 5.5. Risk exposure percentages denote the percentage of the total time considered (i.e., selected using the time window slider) during which a subject is under an "Acceptable" or "Not Recommended" condition for a specific DoF. Additionally, risk exposure occurrences represent the number of instances a worker is exposed to a risky posture within the considered time interval. Finally, "Risk and Exposure" pertains to the entire time and not just the selected portion, presenting the percentage of time a worker is subjected to postures considered in EAWS, along with the associated risk score for each posture.

Figure 5.8 corresponds to the metric section presented under the "Posture Segment" segmentation type. The data presented mirrors that for the "Label of Risk" segmentation depicted in Figure 5.7, with the inclusion of the "Exposure Percentage" indicating the percentage of time spent by a worker in the angular conditions depicted in the visualisations presented in Figure 5.6.

The developed dashboard presents the angle over time plot of the body segment as the SoterTask

Figure 5.6: Dashboard's section for data visualisation. The data refers to the trunk and the segmentation presented is based on angular limits ("Posture Segment").

and inSEER software, but taking it a step further and presenting this for each DoF. Additionally, the segmentation is performed by vertical coloured bars over the graph according to ISO 11226, allowing easier identification of risky and not risky postures for certain segment. Navigation is enabled in the graphs allowing a more complete and interactive analysis.

SoterTask presents a bar plot regarding the percentage of the total time a specific body section was in a high, medium or no-risk position, while ergoIA presents bar plots regarding the percentage of the total time the worker was in a certain posture, e.g., with arms above the head. The developed dashboard presents tables with the percentage of the total time and the number of instances a worker was in a risky or safe posture, as well as the percentage of time a worker was exposed to specific postures.

BoB software presents the plot of worksheet scores over time, while the dashboard presents the EAWS scores in a detailed table regarding the total work cycle considered. This offers insights regarding different segments and postures contributing to the comprehensive evaluation of the complete work cycle.

To comprehend and address the constraints faced by ergonomists regarding risk assessment at Autoeuropa, the developed dashboard is discussed in the following section.

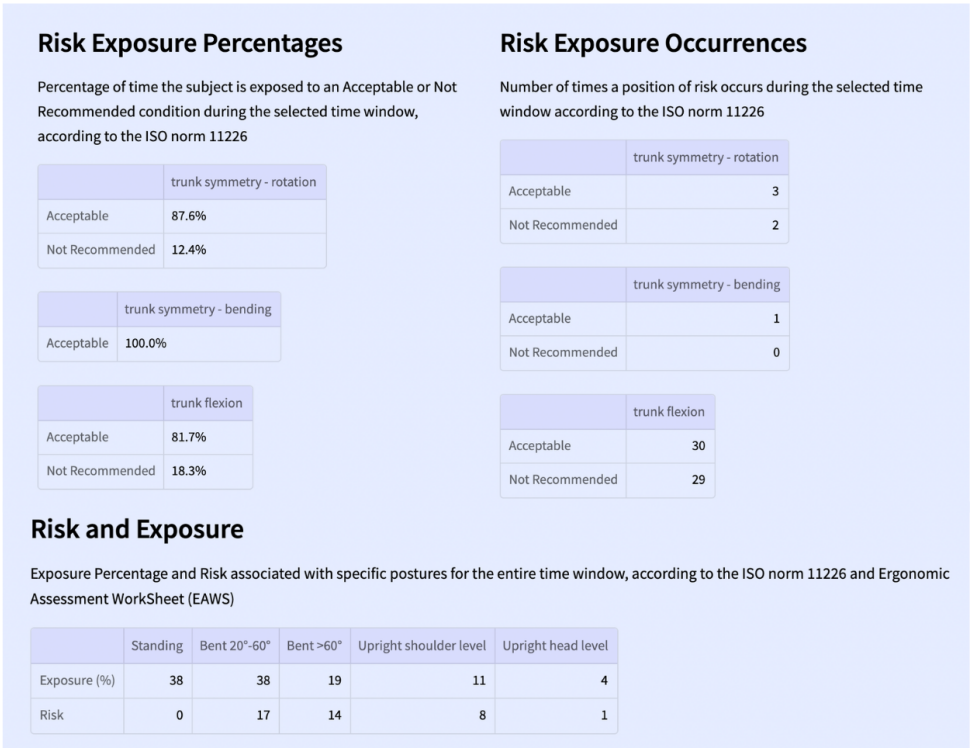

Risk Exposure Percentages

Percentage of time the subject is exposed to an Acceptable or Not Recommended condition during the selected time window, according to the ISO norm 11226

	trunk symmetry - rotation
Acceptable	87.6%
Not Recommended	12.4%

	trunk symmetry - bending
Acceptable	100.0%

	trunk flexion
Acceptable	81.7%
Not Recommended	18.3%

Risk Exposure Occurrences

Number of times a position of risk occurs during the selected time window according to the ISO norm 11226

	trunk symmetry - rotation
Acceptable	3
Not Recommended	2

	trunk symmetry - bending
Acceptable	1
Not Recommended	0

	trunk flexion
Acceptable	30
Not Recommended	29

Risk and Exposure

Exposure Percentage and Risk associated with specific postures for the entire time window, according to the ISO norm 11226 and Ergonomic Assessment WorkSheet (EAWS)

	Standing	Bent 20°-60°	Bent >60°	Upright shoulder level	Upright head level
Exposure (%)	38	38	19	11	4
Risk	0	17	14	8	1

Figure 5.7: Dashboard's metrics section. The presented data refers to the trunk regarding a segmentation based ISO 11226 ("Label of Risk").

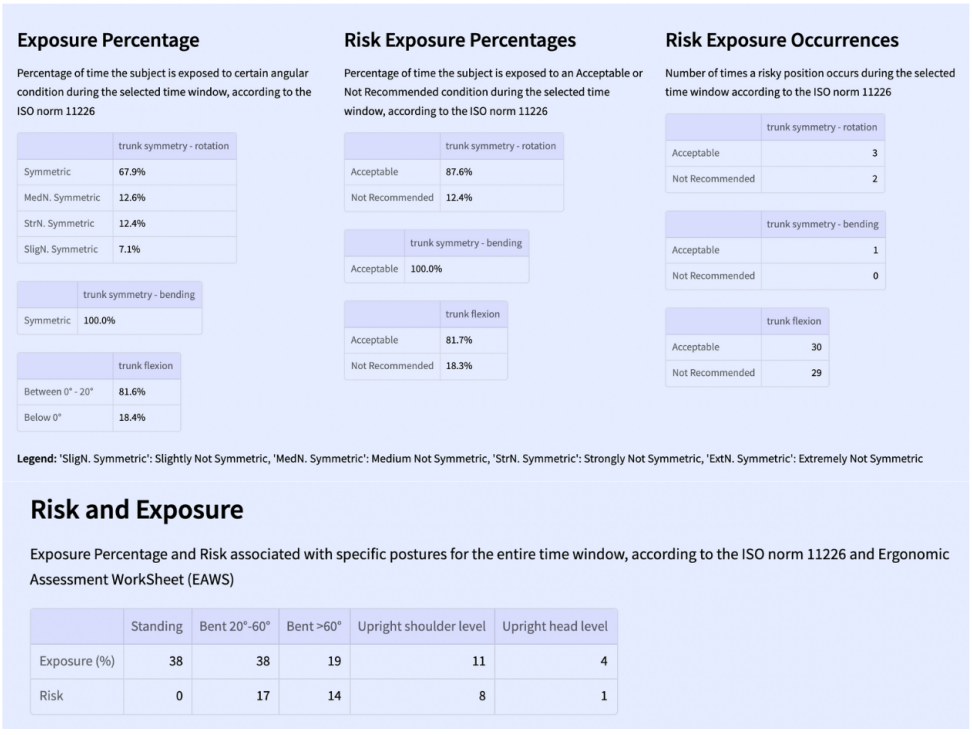

Exposure Percentage

Percentage of time the subject is exposed to certain angular condition during the selected time window, according to the ISO norm 11226

	trunk symmetry - rotation
Symmetric	67.9%
MedN. Symmetric	12.6%
StrN. Symmetric	12.4%
SligN. Symmetric	7.1%

	trunk symmetry - bending
Symmetric	100.0%

	trunk flexion
Between 0° - 20°	81.6%
Below 0°	18.4%

Risk Exposure Percentages

Percentage of time the subject is exposed to an Acceptable or Not Recommended condition during the selected time window, according to the ISO norm 11226

	trunk symmetry - rotation
Acceptable	87.6%
Not Recommended	12.4%

	trunk symmetry - bending
Acceptable	100.0%

	trunk flexion
Acceptable	81.7%
Not Recommended	18.3%

Risk Exposure Occurrences

Number of times a risky position occurs during the selected time window according to the ISO norm 11226

	trunk symmetry - rotation
Acceptable	3
Not Recommended	2

	trunk symmetry - bending
Acceptable	1
Not Recommended	0

	trunk flexion
Acceptable	30
Not Recommended	29

Legend: 'SligN. Symmetric': Slightly Not Symmetric, 'MedN. Symmetric': Medium Not Symmetric, 'StrN. Symmetric': Strongly Not Symmetric, 'ExtN. Symmetric': Extremely Not Symmetric

Risk and Exposure

Exposure Percentage and Risk associated with specific postures for the entire time window, according to the ISO norm 11226 and Ergonomic Assessment WorkSheet (EAWS)

	Standing	Bent 20°-60°	Bent >60°	Upright shoulder level	Upright head level
Exposure (%)	38	38	19	11	4
Risk	0	17	14	8	1

Figure 5.8: Dashboard's metrics section. The presented data refers to the trunk regarding a segmentation based on angular limits ("Posture Segment").

5.2.3 Implications for Ergonomists' Practice

In this project, the arduous and manual process of completing the EAWS is automated through acquisitions using IMU data. This automation significantly reduces the time and effort expended by ergonomists, who would otherwise be limited to subjective visual analyses or repetitive reviews of video records. The dashboard displays EAWS scores for the relevant postures, as illustrated in Figures 5.7 and 5.8.

However, more in-depth analysis and comprehensive evaluation become challenging when relying solely on data filled through EAWS, particularly without visual support. This is where the dashboard's primary visual support becomes valuable, providing ergonomists with interactive visualisations of the angle over time for each DoF. This feature allows for analyses employing various segmentation types, time windows, and body segments, as depicted in Figures 5.5 and 5.6.

Addressing the difficulties and needs of ergonomists outlined in Table 5.5, the visualisations in Figure 5.5 enable, with a quick visual assessment, the identification of instances with extreme postures throughout the work cycle(s), as well as pinpointing these occurrences. By recognizing significant or frequent coloured segments, typically in red or purple, ergonomists gain a general understanding of workers' exposure to risk postures.

Recognizing that maintaining a posture without an extreme angle for an extended period can also pose a risk to developing WRMSDs, the graphs presented in Figure 5.6 offer angular segmentations. These visualisations serve to identify working postures that, while not having a pronounced angle, are sustained for significant durations.

When the graphical visualisations are coupled with the tables showcased in Figures 5.7 and 5.8, additional evaluations become feasible. This includes pinpointing risk postures flagged as problematic and determining the associated workstations for these risks. The ultimate aim is to prevent placing injured workers in such workstations or designing work sequences that minimize excessive strain on specific body segments.

For instance, through a comparative analysis of risk graphs concerning the right shoulder assessment of the same worker at two distinct workstations, ergonomists can initially discern variations in the risk exposure patterns. This assessment helps in determining which workstation exhibits a higher prevalence of not recommended postures for this specific body segment, following the ISO guidelines. Subsequently, ergonomists can refer to the metrics tables to identify significant differences in the duration of risk posture exposure or the number of repetitions for a risk posture in each work setting. Additionally, the EAWS risk scores contribute to this evaluative process.

This approach facilitates workstation comparisons specific to a body segment, aiding in the identification of the riskiest workstations for an individual worker or the workforce in general. Furthermore, it enables evaluations across entire sequences of workstations, assisting in establishing an optimal order for workstation rotations that minimize the overall risk.

Personalizing the assessment and work environment for each worker becomes crucial, particularly when contemplating the option of enabling workers, who would typically be sent home, to continue working in conditions conducive to productivity. For example, employees with shoulder injuries can be prevented from engaging in tasks that require arm movements above shoulder level. Instead of resorting to a work suspension, these individuals can be accommodated in workstations and rotations specifically designed to minimize their risk exposure. This approach serves the dual purpose of ensuring the worker's well-being and maintaining overall productivity in the factory.

Moreover, the visualisations and metrics provided by the dashboard offer a valuable tool for compar-

ing workers. This aspect gains significance as experience may influence postural efficiency and exposure to risk. In cases where workers exhibit heightened risk during certain tasks, training interventions can be considered to address these concerns, making the dashboard a versatile resource for workforce management and optimization.

5.2.4 Dashboard Limitations

The implemented dashboard has certain limitations. Firstly, it lacks a built-in feature facilitating direct comparative analysis between two or more work cycles, workstations or even sequences of workstations. Additionally, continuous monitoring of workers, involving the storage of previous ergonomic assessments for comparison, is not directly supported by the dashboard. Furthermore, the dashboard does not provide general statistics for a worker's ergonomic assessment over time, nor does it allow simultaneous analysis of different workers, hindering capabilities like workstation analysis. These aspects represent areas for potential future development.

Chapter 6

Conclusions and Future Work

In the era of Industry 4.0 and 5.0, the industrial landscape has undergone a significant digital transformation, aligning with a human-centric approach to enhance sustainable productivity. Within automotive assembly lines, the prevalence of WRMSDs is heightened due to factors such as awkward postures, repetitive movements, and the handling of heavy objects. These challenges predominantly impact the upper limbs of workers.

The OPERATOR project is strategically focused on the digitalisation of job quality assessment, leveraging technology to proactively address ergonomic risks and, ultimately, safeguard the health and well-being of workers. This thesis addresses the challenge of detecting awkward upper body postures using IMU data, while also exploring visualisation issues faced by ergonomists during risk assessments.

The initial hurdle arises from the limitation of relying solely on joint angles for accurate posture classification, particularly for intricate postures at the shoulder level or overhead work. Consequently, this thesis concentrates on enhancing the risk assessment at Autoeuropa, by specifically targeting these two challenging postures.

Despite employing various ML classifiers, the obtained results lacked satisfaction and generalizability for the intended detection of the specific working postures. Consequently, a CNN model was developed, achieving recall scores of 0.95 and 0.97 at the shoulder level and overhead working postures, respectively. A macro average F1-score of 0.96 was attained using 35 features, mirroring the achievement of a study that tackled the same task but employed 69 features.

For the second problem addressed in this thesis, the classification model serves as input for algorithms that perform data segmentation based on both EAWS and ISO norm 11226. This segmented data then fuels a dashboard designed to enhance data visualisation, ultimately contributing to the risk assessment process and supporting ergonomists' tasks at Autoeuropa.

Considering the significant impact of the work conducted in ergonomic risk assessment, ultimately contributing to the prevention and recovery of musculoskeletal injuries, especially within the context of Autoeuropa, the next step involves validating the model with specific data collected from the assembly line and testing the dashboard feasibility and usability with end-users. The transition from public database data to case-specific study data is crucial to confirm the practical application and effectiveness of the developed tools. This adaptation could be facilitated by employing transfer learning techniques, utilizing the knowledge gained from the pre-trained network on the AnDy dataset for the assembly line collected data. Additionally, one other possible facilitator is the usage of the same data collection system in the AnDy dataset as well as at Autoeuropa.

Furthermore, adapting the dashboard to enable a direct and automated comparison between workstations, job rotations, and even different workers aims to enhance and further optimize the efforts of

ergonomists in preventing musculoskeletal injuries.

Taking a broader perspective, future work involves developing methods to design assembly lines that proactively minimize risks. The current methodologies discussed in this dissertation are primarily applicable to further optimise existing assembly lines, emphasizing the need for proactive risk reduction strategies in assembly line design.

Bibliography

[1] CCOHS. *Work-related Musculoskeletal Disorders (WMSDs) - CCOHS*. https://www.ccohs.ca/oshanswers/diseases/rmirsi.html. Accessed: 07/07/2023. Last Updated: 13/06/2023.

[2] Hamizatun Binti Mohd Fazi, Nik Mohd Zuki B Nik Mohamed, and Azizul Qayyum Bin Basri. "Risks assessment at automotive manufacturing company and ergonomic working condition". In: *IOP Conference Series: Materials Science and Engineering*. Vol. 469. 1. IOP Publishing. 2019, p. 012106.

[3] Antonio Sousa-Uva et al. *Lesões musculoesqueléticas relacionadas com o trabalho: guia para a prevenção*. May 2008.

[4] Sandul Yasobant and Paramasivan Rajkumar. "Work-related musculoskeletal disorders among health care professionals: A cross-sectional assessment of risk factors in a tertiary hospital, India". In: *Indian journal of occupational and environmental medicine* 18.2 (2014), p. 75.

[5] Geoffrey C David. "Ergonomic methods for assessing exposure to risk factors for work-related musculoskeletal disorders". In: *Occupational medicine* 55.3 (2005), pp. 190–199.

[6] United Nations. *THE 17 GOALS | Sustainable Development*. https://sdgs.un.org/goals, note = Accessed: 03/01/2024.

[7] Zofia Gródek-Szostak et al. "From Industry 4.0 Paradigm Towards Industry 5.0". In: *ENVIRONMENT. TECHNOLOGIES. RESOURCES. Proceedings of the International Scientific and Practical Conference*. Vol. 2. 2023, pp. 46–49.

[8] Bader Alojaiman. "Technological Modernizations in the Industry 5.0 Era: A Descriptive Analysis and Future Research Directions". In: *Processes* 11.5 (2023), p. 1318.

[9] Alexey Yu Zalozhnev and Vasily N Ginz. "Industry 4.0: Underlying Technologies. Industry 5.0: Human-Computer Interaction as a Tech Bridge from Industry 4.0 to Industry 5.0". In: *2023 9th International Conference on Web Research (ICWR)*. IEEE. 2023, pp. 232–236.

[10] Jan de Kok et al. *Work-related musculoskeletal disorders: prevalence, costs and demographics in the EU*. Nov. 2019.

[11] Akram Sadat Jafari Roodbandi et al. "Prevalence of musculoskeletal disorders and posture assessment by qec and inter-rater agreement in this method in an automobile assembly factory: Iran-2016". In: *Proceedings of the 20th Congress of the International Ergonomics Association (IEA 2018) Volume VIII: Ergonomics and Human Factors in Manufacturing, Agriculture, Building and Construction, Sustainable Development and Mining 20*. Springer. 2019, pp. 333–339.

[12] Stephen Bevan. "Economic impact of musculoskeletal disorders (MSDs) on work in Europe". In: *Best Practice & Research Clinical Rheumatology* 29.3 (2015), pp. 356–373.

[13] Luıs Cunha-Miranda, Filomena Carnide, and M Fátima Lopes. "PREVALENCE OF RHEUMATIC OCCUPATIONAL DISEASES–PROUD STUDY." In: *Acta reumatologica portuguesa* 35.2 (2010).

[14] M Guerreiro et al. "An analysis on neck and upper limb musculoskeletal symptoms in Portuguese automotive assembly line workers". In: *International Journal of Occupational and Environmental Safety* 1.1 (2017), pp. 59–68.

[15] Marisa M Guerreiro et al. "Self-Reported variables as determinants of upper limb musculoskeletal symptoms in assembly line workers". In: *Safety and Health at Work* 11.4 (2020), pp. 491–499.

[16] Robert A Werner et al. "A longitudinal study of industrial and clerical workers: predictors of upper extremity tendonitis". In: *Journal of occupational rehabilitation* 15 (2005), pp. 37–46.

[17] R. Ellegast et al. *Assessment of physical workloads to prevent work-related MSDs*. OSHwiki, 2023. DOI: https://oshwiki.osha.europa.eu/en/themes/assessment-physical-workloads-prevent-work-related-msds.

[18] Center for Assistive Information Fraunhofer Portugal and Communication Solutions – AICOS. *OPERATOR*. https://www.aicos.fraunhofer.pt/en/work/projects/operator.html. Accessed: 01/12/2023. 2020.

[19] Junqi Zhao and Esther Obonyo. "Applying incremental Deep Neural Networks-based posture recognition model for ergonomics risk assessment in construction". In: *Advanced Engineering Informatics* 50 (2021), pp. 101–374.

[20] E. A. Spencer, J. Brassey, and K. Mahtani. *Recall bias*. Accessed: 07/01/2024. 2017. URL: https://catalogofbias.org/biases/recall-bias/.

[21] Maria Grazia Lourdes Monaco et al. "Work-related upper limb disorders and risk assessment among automobile manufacturing workers: A retrospective cohort analysis". In: *Work* 64.4 (2019), pp. 755–761.

[22] Ahmed Humadi et al. "In-field instrumented ergonomic risk assessment: Inertial measurement units versus Kinect V2". In: *International Journal of Industrial Ergonomics* 84 (2021), p. 103147.

[23] Lorenzo Peppoloni et al. "A novel wearable system for the online assessment of risk for biomechanical load in repetitive efforts". In: *International Journal of Industrial Ergonomics* 52 (2016), pp. 1–11.

[24] Woojoo Kim et al. "Comparison of joint angle measurements from three types of motion capture systems for ergonomic postural assessment". In: *Advances in Physical, Social & Occupational Ergonomics: Proceedings of the AHFE 2020 Virtual Conferences on Physical Ergonomics and Human Factors, Social & Occupational Ergonomics and Cross-Cultural Decision Making, July 16–20, 2020, USA*. Springer. 2020, pp. 3–11.

[25] Oguz Akkas et al. "Measuring exertion time, duty cycle and hand activity level for industrial tasks using computer vision". In: *Ergonomics* 60.12 (2017), pp. 1730–1738.

[26] Li Li, Tara Martin, and Xu Xu. "A novel vision-based real-time method for evaluating postural risk factors associated with musculoskeletal disorders". In: *Applied Ergonomics* 87 (2020), p. 103138.

[27] Simona Salicone et al. “Low-cost real-time motion capturing system using inertial measurement units”. In: *ACTA IMEKO* 11.3 (2022), pp. 1–9.

[28] Maria Cornacchia et al. “A survey on activity detection and classification using wearable sensors”. In: *IEEE Sensors Journal* 17.2 (2016), pp. 386–403.

[29] Sen Qiu et al. “Multi-sensor information fusion based on machine learning for real applications in human activity recognition: State-of-the-art and research challenges”. In: *Information Fusion* 80 (2022), pp. 241–265.

[30] Ferhat Attal et al. “Physical human activity recognition using wearable sensors”. In: *Sensors* 15.12 (2015), pp. 31314–31338.

[31] Amit Hirawat, Swapnesh Taterh, and Tarun Kumar Sharma. “A dynamic window-size based segmentation technique to detect driver entry and exit from a car”. In: *Journal of King Saud University-Computer and Information Sciences* 34.10 (2022), pp. 8514–8522.

[32] Oresti Banos et al. “Window size impact in human activity recognition”. In: *Sensors* 14.4 (2014), pp. 6474–6499.

[33] Mst Alema Khatun et al. “Deep CNN-LSTM with self-attention model for human activity recognition using wearable sensor”. In: *IEEE Journal of Translational Engineering in Health and Medicine* 10 (2022), pp. 1–16.

[34] Kun Xia, Jianguang Huang, and Hanyu Wang. “LSTM-CNN architecture for human activity recognition”. In: *IEEE Access* 8 (2020), pp. 56855–56866.

[35] Francisco Javier Ordóñez and Daniel Roggen. “Deep convolutional and lstm recurrent neural networks for multimodal wearable activity recognition”. In: *Sensors* 16.1 (2016), p. 115.

[36] Ilaria Conforti et al. “Measuring biomechanical risk in lifting load tasks through wearable system and machine-learning approach”. In: *Sensors* 20.6 (2020), p. 1557.

[37] Seyed Mohammadreza Hosseinian et al. “Static and dynamic work activity classification from a single accelerometer: Implications for ergonomic assessment of manual handling tasks”. In: *IISE Transactions on Occupational Ergonomics and Human Factors* 7.1 (2019), pp. 59–68.

[38] Hao-Yuan Tang et al. “Upper body posture recognition using inertial sensors and recurrent neural networks”. In: *Applied Sciences* 11.24 (2021), p. 12101.

[39] Adrien Malaisé et al. “Activity recognition for ergonomics assessment of industrial tasks with automatic feature selection”. In: *IEEE Robotics and Automation Letters* 4.2 (2019), pp. 1132–1139.

[40] Pauline Maurice et al. *Andydata-Lab-onePerson*. Jan. 2022. URL: `https://zenodo.org/records/3254403`.

[41] Burcu Felekoglu and Seren Ozmehmet Tasan. “Interactive ergonomic risk mapping: A practical approach for visual management of workplace ergonomics”. In: *International Journal of Occupational Safety and Ergonomics* 28.1 (2022), pp. 45–61.

[42] David Kostolani, Michael Wollendorfer, and Sebastian Schlund. “ErgoMaps: Towards Interpretable and Accessible Automated Ergonomic Analysis”. In: *2022 IEEE 3rd International Conference on Human-Machine Systems (ICHMS)*. IEEE. 2022, pp. 1–7.

[43] Walentin Heft, Linda Pfeiffer, and Paul Rosenthal. “Visualizing Ergonomic Data of Industrial Work Processes: A Design Study.” In: *VISIGRAPP (3: IVAPP)*. 2017, pp. 274–282.

[44] Guangyan Li and Peter Buckle. "Current techniques for assessing physical exposure to work-related musculoskeletal risks, with emphasis on posture-based methods". In: *Ergonomics* 42.5 (1999), pp. 674–695.

[45] *SoterTask - Ergonomic Risk Task Assessment App*. Accessed: 22/02/2024. URL: https://soteranalytics.com/solutions/sotertask.

[46] *Inseer: Ergonomic Assessment Software*. Accessed: 22/02/2024. URL: https://inseer.com/Content/Our-Solution.cfm.

[47] *HOME - ergoIA*. Accessed: 22/02/2024. URL: https://ergoia.net/?lang=en.

[48] *ErgoPlus*. Accessed: 22/02/2024. URL: https://ergo-plus.com/software/.

[49] *BoB/Ergo*. Accessed: 22/02/2024. URL: https://www.bob-biomechanics.com/bob-4-ergo/.

[50] Duane V Knudson and D Knudson. *Fundamentals of biomechanics*. Vol. 183. Springer, 2007.

[51] *Ergonomics – Evaluation of StaticWorking Postures*. Standard. Geneva, CH: International Organization for Standardization, 2000.

[52] Michela Dalle Mura and Gino Dini. "Optimizing ergonomics in assembly lines: A multi objective genetic algorithm". In: *CIRP Journal of Manufacturing Science and Technology* 27 (2019), pp. 31–45.

[53] Waldemar Karwowski. "The discipline of ergonomics and human factors". In: *Handbook of human factors and ergonomics* (2006), pp. 1–31.

[54] International Ergonomics Association. *What Is Ergonomics (HFE)?* https://iea.cc/about/what-is-ergonomics/. Accessed: 07/01/2024. Last Updated: 30/12/2022.

[55] Alena Otto and Olga Battaıa. "Reducing physical ergonomic risks at assembly lines by line balancing and job rotation: A survey". In: *Computers & Industrial Engineering* 111 (2017), pp. 467–480.

[56] Michela Dalle Mura and Gino Dini. "Improving ergonomics in mixed-model assembly lines balancing noise exposure and energy expenditure". In: *CIRP Journal of Manufacturing Science and Technology* 40 (2023), pp. 44–52.

[57] A Pimparel et al. "How ergonomic evaluations influence the risk of musculoskeletal disorders in the industrial context? a brief literature review". In: *Occupational and Environmental Safety and Health III* (2022), pp. 399–409.

[58] Karlheinz Schaub et al. "The European assembly worksheet". In: *Theoretical Issues in Ergonomics Science* 14.6 (2013), pp. 616–639.

[59] Maria Lua Nunes et al. "Posture Risk Assessment in an Automotive Assembly Line Using Inertial Sensors". In: *IEEE Access* 10 (2022), pp. 83221–83235.

[60] Matteo Menolotto et al. "Motion capture technology in industrial applications: A systematic review". In: *Sensors* 20.19 (2020), p. 5687.

[61] Sani Salisu et al. "Motion Capture Technologies for Ergonomics: A Systematic Literature Review". In: *Diagnostics* 13.15 (2023), p. 2593.

[62] Sol Lim and Clive D'Souza. "A narrative review on contemporary and emerging uses of inertial sensing in occupational ergonomics". In: *International journal of industrial ergonomics* 76 (2020), p. 102937.

[63] Nuno Oliveira, Joonsun Park, and Peter Barrance. “Using inertial measurement unit sensor single axis rotation angles for knee and hip flexion angle calculations during gait”. In: *IEEE Journal of Translational Engineering in Health and Medicine* 11 (2022), pp. 80–86.

[64] Muhammad Yahya et al. “Motion capture sensing techniques used in human upper limb motion: A review”. In: *Sensor Review* 39.4 (2019), pp. 504–511.

[65] Caiming Zhang and Yang Lu. “Study on artificial intelligence: The state of the art and future prospects”. In: *Journal of Industrial Information Integration* 23 (2021), p. 100224.

[66] Orkun Baloglu, Samir Q Latifi, and Aziz Nazha. “What is machine learning?” In: *Archives of Disease in Childhood-Education and Practice* (2021).

[67] IBM. *What is machine learning?* `https://www.ibm.com/topics/machine-learning#toc-challenges-L8chLUzD`. Accessed: 13/01/2024.

[68] Jyotismita Talukdar, Thipendra P Singh, and Basanta Barman. “Supervised Learning”. In: *Artificial Intelligence in Healthcare Industry*. Springer, 2023, pp. 51–86.

[69] Dirk Valkenborg et al. “Unsupervised learning”. In: *American Journal of Orthodontics and Dentofacial Orthopedics* 163.6 (2023), pp. 877–882.

[70] Attiano Purpura-Pontoniere et al. “Semi-Supervised Relational Contrastive Learning”. In: *arXiv preprint arXiv:2304.05047* (2023).

[71] Guolin Zheng et al. “Semi-supervised Learning with Nearest-Neighbor Label and Consistency Regularization”. In: *International Conference on Machine Learning for Cyber Security*. Springer. 2022, pp. 144–154.

[72] “Applying Decision Tree Algorithm Classification and Regression Tree (CART) Algorithm to Gini Techniques Binary Splits”. In: vol. 12. 5. 2023, pp. 77–81. DOI: `10.35940/ijeat.e4195.0612523`.

[73] Andreas C Muller and Sarah Guido. *Introduction to machine learning with Python*. O’Reilly, 2017, pp. 68–118, 251–296.

[74] Leonardo Vanneschi and Sara Silva. “Support Vector Machines”. In: *Lectures on Intelligent Systems*. Springer, 2023, pp. 271–281.

[75] YuXuan Shi and HongLi Xu. “The Iris Cassification Based on Gaussian Naive Bayes Agorithm”. In: *Proceedings of the 2022 6th International Conference on Electronic Information Technology and Computer Engineering*. 2022, pp. 732–736.

[76] “Heart Failure Prediction using Gaussian Naïve Bayes Algorithm”. In: 2023, pp. 125–143. DOI: `10.36548/jitdw.2023.2.004`.

[77] Li Yang and Abdallah Shami. “On hyperparameter optimization of machine learning algorithms: Theory and practice”. In: *Neurocomputing* 415 (2020), pp. 295–316.

[78] Drew Wilimitis and Colin G Walsh. “Practical Considerations and Applied Examples of Cross-Validation for Model Development and Evaluation in Health Care: Tutorial”. In: *JMIR AI* (2023).

[79] Sarat Kumar Sarvepalli. “Deep learning in neural networks: the science behind an artificial brain”. In: *Liverpool Hope University, Liverpool* (2015).

[80] N. McCullum. *Deep Learning Neural Networks explained in plain English*. `https://www.freecodecamp.org/news/deep-learning-neural-networks-explained-in-plain-english`. Accessed: 13/01/2024. Last Updated: 28/04/2021.

[81] Su-Hyun Han et al. “Artificial neural network: understanding the basic concepts without mathematics”. In: *Dementia and Neurocognitive Disorders* 17.3 (2018), pp. 83–89.

[82] Ajay Shrestha and Ausif Mahmood. “Review of deep learning algorithms and architectures”. In: *IEEE access* (2019).

[83] Aurélien Géron. *Hands-on machine learning with Scikit-Learn, Keras, and TensorFlow*. " O’Reilly Media, Inc.", 2022, pp. 279–292.

[84] Accessed: 21/01/2024. Dec. 2022. URL: `https://deepchecks.com/glossary/learning-rate-in-machine-learning/`.

[85] Tingting Wu, Peng Zeng, and Chunhe Song. “An optimization Strategy for Deep Neural Networks Training”. In: *2022 International Conference on Image Processing, Computer Vision and Machine Learning (ICICML)*. IEEE. 2022, pp. 596–603.

[86] Jason Brownlee. *Gentle introduction to the adam optimization algorithm for deep learning*. Accessed: 21/01/2024. Jan. 2021. URL: `https://machinelearningmastery.com/adam-optimization-algorithm-for-deep-learning/`.

[87] Chigozie Nwankpa et al. “Activation functions: Comparison of trends in practice and research for deep learning”. In: *arXiv preprint arXiv:1811.03378* (2018).

[88] D. Shah. *Cross Entropy Loss: Intro, Applications, Code - V7 Labs*. `https://www.v7labs.com/blog/cross-entropy-loss-guide`. Accessed: 1/01/2024. Last Updated: 28/04/2021.

[89] Neena Aloysius and M Geetha. “A review on deep convolutional neural networks”. In: *2017 international conference on communication and signal processing (ICCSP)*. IEEE. 2017, pp. 0588–0592.

[90] Bendong Zhao et al. “Convolutional neural networks for time series classification”. In: *Journal of Systems Engineering and Electronics* 28.1 (2017), pp. 162–169.

[91] Qiuhong Ke et al. “Computer vision for human–machine interaction”. In: *Computer Vision for Assistive Healthcare*. Elsevier, 2018, pp. 127–145.

[92] Purwono Purwono et al. “Understanding of convolutional neural network (cnn): A review”. In: *International Journal of Robotics and Control Systems* 2.4 (2022), pp. 739–748.

[93] Elsa Chaerun Nisa and Yean-Der Kuan. “Comparative assessment to predict and forecast water-cooled chiller power consumption using machine learning and deep learning algorithms”. In: *Sustainability* 13.2 (2021), p. 744.

[94] Kwetishe Joro Danjuma. “Performance evaluation of machine learning algorithms in post-operative life expectancy in the lung cancer patients”. In: *arXiv preprint arXiv:1504.04646* (2015).

[95] Mohammad Hossin and Md Nasir Sulaiman. “A review on evaluation metrics for data classification evaluations”. In: *International journal of data mining & knowledge management process* 5.2 (2015), p. 1.

[96] Kayley Marshall. *How to use the AUC ROC curve for the multi-class model?* Accessed:16/04/2024. Mar. 2023. URL: `https://deepchecks.com/question/how-to-use-the-auc-roc-curve-for-the-multi-class-model/`.

[97] Maria Lua de Coelho Nunes. *Quantifying the Ergonomic Risk and Biomechanical Exposure in Automotive Assembly Lines*. 2021.

[98] Pauline Maurice et al. “Human movement and ergonomics: An industry-oriented dataset for collaborative robotics”. In: *The International Journal of Robotics Research* 38.14 (2019), pp. 1529–1537.

[99] Marılia Barandas et al. “TSFEL: Time series feature extraction library”. In: *SoftwareX* 11 (2020), p. 100456.

[100] PhD Brinnae Bent. *Step-by-step guide to leave-one-person-out cross validation with random forests in Python*. Accessed: 20/01/2024. June 2020. URL: https://medium.com/analytics-vidhya/step-by-step-guide-to-leave-one-person-out-cross-validation-with-random-forests-in-python-34b2eaefb628.

[101] Ross Brancati. *Leave one subject out cross validation for Machine Learning Models*. Accessed: 20/01/2024. Feb. 2023. URL: https://ai.plainenglish.io/leave-one-subject-out-cross-validation-for-machine-learning-model-557a09c7891d.

[102] *sklearn.utils.class*$_w$*eight.compute*$_c$*lass*$_w$*eight*. Accessed: 22/02/2024. URL: https://scikit-learn.org/stable/modules/generated/sklearn.utils.class_weight.compute_class_weight.html.

[103] U Myn, M Link, and M Awinda. “Xsens mvn user manual”. In: *Xsens Motion Technologies BV: Enschede, The Netherlands* (2015).

Appendix A

State-of-the-Art

Table A.1: Description of the MHEALTH, UCI-HAR, H-Activity, WISDM, OPPORTUNITY and Skoda datasets, according to the types and locations of the sensors used, as well as the activities or gestures annotated in the dataset.

Dataset	Sensor Type	Sensor Location	Activity/Gesture	
MHEALTH	Wearable sensor: Accelerometer Gyroscope Magnetometer	Chest Right wrist Left ankle	Standing still Sitting and relaxing Lying down Walking Climbing stairs Waist bends forward	Frontal elevation of arms Knees bending (crouching) Cycling Jogging Running Jump front and back
UCI-HAR	Smartphone: Accelerometer Gyroscope	Waist	Walking Walking Upstairs Walking Downstairs	Sitting Standing Laying
H-Activity	Smartphone: Accelerometer Gyroscope Linear Acceleration	Right trousers pocket	Sitting/Standing Walking Jogging Running	
WISDM	Smartphone and smartwatch: Accelerometer Gyroscope	Smartphone on pocket and smartwatch in dominant hand	Walking Jogging Stairs Sitting Standing Typing Brushing Teeth Eating Soup Eating Chips	Eating Pasta Drinking from Cup Eating Sandwich Kicking (Soccer Ball) Playing Catch w/ Tennis Ball Dribbling (Basketball) Writing Clapping Folding Clothes
OPPORTUNITY	Body-worn sensors: Inertial measurement units, 3D acceleration sensors, 3D localization information	Entire body	Open and Close Door Open and Close Fridge Open and Close Dishwasher Open and Close Drawer	Clean Table Drink from Cup Toggle Switch Null
Skoda	3D acceleration sensors	Arms	Write on Notepad Open and Close Hood Check Gaps Door Open and Close Door	Check Steering Wheel Open and Close Trunk Check Trunk

Appendix B

Theoretical Background

Figure B.1: MVN Link Lycra suit (from [103]). This suit has 17 sensors: 1 sensor on the head, sternum and pelvis, and 1 sensor on each scapula, upper arm, forearm, hand, thigh, shank and foot.

Appendix C

Materials and Methods

EAWS Pro-forma Sheet Assessment

The risk score can be computed according to the rating scale proposed in the pro-forma sheet EAWS.
It was implemented an adapted EAWS of the table "Basic Positions / Postures and movements of trunk and arms (per shift)", particularly of its section "Standing (and Walking)".

BASIC POSITIONS / POSTURES AND MOVEMENTS OF TRUNK AND ARMS (PER SHIFT), STANDING (AND WALKING) SECTION

Basic Positions / Postures and movements of trunk and arms (per shift)													Postures			
(incl. loads of <3 kg and action forces of 30-40 N) Static postures: > 4sec High frequency movements: 2 trunk bending or 10 arm lifting > 60° per min			Evaluation of static postures and/or high frequent movements of trunk/arms Duration [sec/min] = duration of posture(s) x 60 / cycle time										Sum of lines	Asymmetry effects Trunk Rotation 1)	Lateral Bending 1)	Far Reach 2)
		[%]	5	7,5	10	15	20	27	33	50	67	83		int dur 0-5 0-3 Intensity x Duration	int dur 0-5 0-3 Intensity x Duration	int dur 0-5 0-2 Intensity x Duration
		[sec/min]	3	4,5	6	9	12	16	20	30	40	50				
		[min/8h]	24	36	48	72	96	130	160	240	320	400				
Standing (and walking)																
1		Standing & walking in alteration, standing with support	0	0	0	0	0,5	1	1	1	1,5	2				
2		Standing, no body support (for other restrict. see Extra Points)	0,7	1	1,5	2	3	4	6	8	11	13				
3		Bent forward (20-60°)	2	3	5	7	9,5	12	18	23	32	40				
		with suitable support	1,3	2	3,5	5	6,5	8	12	15	20	25				
4		Strongly bent forward (>60°)	3,3	5	8,5	12	17	21	30	38	51	63				
		with suitable support	2	3	5	7	9,5	12	18	23	31	38				
5		Upright with elbow at / above shoulder level	3,3	5	8,5	12	17	21	30	38	51	63				
6		Upright with hands above head level	5,3	8	14	19	26	33	47	60	80	100				

Figure 6: Basic positions / postures and movements of trunk and arms - standing (and walking) section.
Note that it was not possible to assess conditions of a few postures, such as static postures with support.

The EAWS's section provides the risk score value for each single condition (row) described in it. Single condition score depends of the percentage of values in data that verify the condition.

SINGLE CONDITIONS

Table 5: Single conditions.

Row	Single Condition	
2	Standing upright	Trunk flexion between 0° and 20°
3	Bent forward	Trunk flexion between 20° and 60°
4	Strongly bent forward	Trunk flexion over 60°
5	Arm abduction over shoulder level	Standing upright × Upper arm abduction over 60°
5	Arm flexion over shoulder level	Standing upright × Upper arm flexion over 60°
6	Hand above head level	Standing upright × Upper arm flexion over 60° × Extreme elbow extension

Figure C.1: Risk assessment guidelines from EAWS, used in the dashboard ([97]).

RISK ASSESSEMENT GUIDELINES

Introduction

This document provides the guidelines used to assess the ergonomic risk associated to the work-method of the operators in Volkswagen Autoeuropa automotive assembly lines. These are based on and adapted from the **International Organisation for Standardisation** (ISO) **norm 11226**, used for the evaluation of static working postures, and the pro-forma sheet ***European Assembly Worksheet*** (EAWS), used in ergonomic risk rating.

Abbreviations

Henceforth, abbreviations, associated to conditions defined in the ISO norm and in the EAWS pro-forma sheet, are adopted in the ergonomic report.

Table 1: Abbreviations adopted in the ergonomic report with regard to ISO norm and EAWS pro-forma sheet.
Note that bent forward is equivalent to trunk flexion.

Abbreviation	Denotation	Based on
TSymRot	Trunk symmetry - rotation	ISO
TSymBend	Trunk symmetry - bending	ISO
TFlex	Trunk flexion	ISO
AwkUA	Awkward upper arm posture	ISO
UAElev	Upper arm elevation	ISO
ExtElbFE	Extreme elbow flexion	ISO
ExtElbPS	Extreme elbow pronation/supination	ISO
ExtWr	Extreme wrist posture	ISO
U	Standing upright	EAWS
BF	Bent forward - 20°-60°	EAWS
BS	Strongly bent forward - over 60°	EAWS
AbduOS	Arm abduction over shoulder level	EAWS
FlexOS	Arm flexion over shoulder level	EAWS
OH	Hand above head level	EAWS
TR	Trunk rotation	EAWS
TB	Trunk bending	EAWS
FR	Far reach	EAWS
SliNS	Slightly not symmetric	EAWS
MedNS	Medium not symmetric	EAWS
StrNS	Strongly not symmetric	EAWS
ExtNS	Extreme not symmetric	EAWS
S	Symmetric	EAWS
100R	100% reaching	EAWS
80R	80% reaching	EAWS
60R	60% reaching	EAWS
ND	Not described (No reaching)	EAWS
UAAbdu	Upper arm abduction over 60°	
UAFlex	Upper arm flexion over 60°	

ISO Norm 11226 Assessment

The ISO Norm 11226 characterises conditions of the upper body segments, in terms of static postures, as "Acceptable" or "Not recommended". Note that being "Acceptable" or "Not recommended", can depend on the holding time in the static posture, i.e. the duration that it is maintained.
The ISO Norm's criteria was considered to be a safe biomechanical exposure characterisation method. Next, the criteria is outlined for trunk, upper arm, forearm and hand segments.

Trunk

Table 2: Conditions for trunk postures.
Trunk symmetry criteria applies to trunk rotation and bending.

Posture Condition	Characterisation
Trunk Symmetry	
Symmetric $< 10°$	Acceptable
Slightly Not Symmetric $\geq 10° \wedge < 15°$	Acceptable
Medium Not Symmetric $\geq 15° \wedge < 25°$	Acceptable
Strongly Not Symmetric $\geq 25° \wedge < 30°$	Not Recommended
Extreme Not Symmetric $\geq 30°$	Not Recommended
Trunk Flexion	
$< 0°$	Not Recommended
$\geq 0° \wedge > 20°$	Acceptable
$\geq 20° \wedge \leq 60°$	Depends on holding time
$> 60°$	Not Recommended

RANGES OF CONDITIONS FOR TRUNK POSTURES

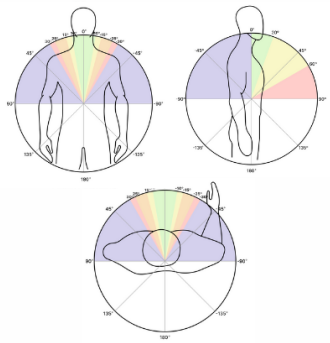

Figure 1: Ranges of conditions for trunk postures: trunk symmetry - bending (top left), trunk flexion (top right) and trunk symmetry - rotation (bottom). Trunk symmetry color scale as symmetric and slightly, medium, strongly and extreme not symmetric. Trunk flexion color scale as Acceptable, Not Recommended and Depends on holding time.

The trunk flexion characterisation for trunk flexion static posture between 20° and 60° depends on holding time as it follows:

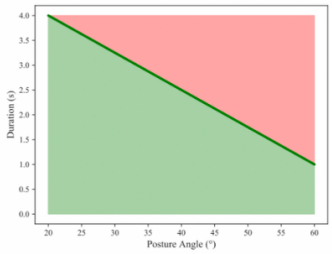

Figure 2: Holding time, and its respective condition that evaluates a static posture. The color scale is as Acceptable and Not Recommended.

Upper Arm

Table 3: Conditions for upper arm postures.
Awkward upper arm posture can be:
1) Arm retroflexion, i.e. elbow behind the trunk when viewed from the side of the trunk;
2) Upper arm adduction, i.e. elbow not visible when viewed from behind the trunk;
3) Extreme upper arm external rotation (90°), i.e. in which "external" refers to an outward rotation around the longitudinal axis of the upper arm with respect to the trunk.
Upper arm elevation refers to upper arm flexion or abduction, which is calculated as the difference between the flexion/abduction angle in the reference posture and the flexion/abduction angle in the static working posture.

Posture Condition	Characterisation
Awkward Upper Arm Posture	
1) Arm retroflexion	Not Recommended
2) Upper arm adduction	Not Recommended
3) Extreme upper arm external rotation	Not Recommended
Upper Arm Elevation	
$\geq 0° \wedge > 20°$	Acceptable
$\geq 20° \wedge \leq 60°$	Depends on holding time
$> 60°$	Not Recommended

RANGES OF CONDITIONS FOR UPPER ARM POSTURES

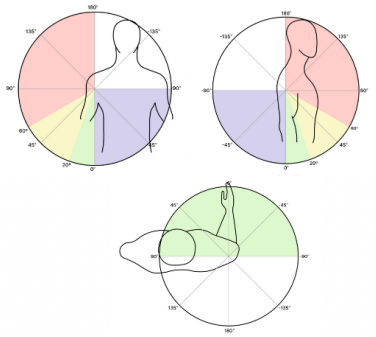

Figure 3: Ranges of conditions for upper arm postures: upper arm abduction/adduction (top left), upper arm extension/flexion (top right) and upper arm inward/outward rotation (bottom). Upper arm rotation color scale as Acceptable. Upper arm abduction/adduction and extension/flexion color scale as Acceptable, Not Recommended and Depends on holding time.

The upper arm elevation (abduction/flexion) characterisation for upper arm elevation (abduction/flexion) static posture between 20° and 60° depends on holding time as in Figure 2.

Forearm and Hand

Table 4: Conditions for forearm and hand postures.
Extreme elbow flexion equals to $\geq 150°$, according to the ISO norm 11226, instead it is used the extreme posture defined in the EAWS ($\geq 60°$).
Extreme forearm pronation/supination equals to $\geq 90°/\geq 60°$, according to the ISO norm 11226, instead it is used the extreme posture defined in the EAWS ($\geq 60°$).
Extreme wrist posture is defined in the ISO norm 11226 norm as:
Wrist flexion: $\leq$ -90° (i.e. extension) $\wedge \geq 90°$ (i.e. flexion);
Wrist deviation: $\leq$ -20° $\wedge \geq 30°$;
instead it is used the extreme posture defined in the EAWS as:
Wrist flexion: $\leq$ -45° (i.e. extension) $\wedge \geq 45°$ (i.e. flexion);
Wrist deviation: $\leq$ -15° $\wedge \geq 20°$.

Posture Condition	Characterisation
Extreme Elbow Flexion	
Elbow flexion $< 60°$	Acceptable
Elbow flexion $\geq 60°$	Not Recommended
Extreme Forearm Pronation/Supination	
Forearm pronation/supination $< 60°$	Acceptable
Forearm pronation/supination $\geq 60°$	Not Recommended
Extreme Wrist Posture	
Wrist deviation $>$ -15° $\wedge <$ 20°	Acceptable
Wrist deviation $\leq$ -15° $\wedge \geq$ 20°	Not Recommended
Wrist flexion $>$ -45° $\wedge <$ 45°	Acceptable
Wrist flexion $\leq$ -45° $\wedge \geq$ 45°	Not Recommended

RANGES OF CONDITIONS FOR FOREARM POSTURES

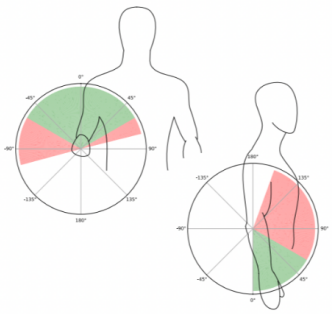

Figure 4: Ranges of conditions for forearm postures: forearm supination/pronation (top left) and elbow flexion (bottom right). Elbow flexion and forearm supination/pronation color scales as Acceptable and Not Recommended.

RANGES OF CONDITIONS FOR HAND POSTURES

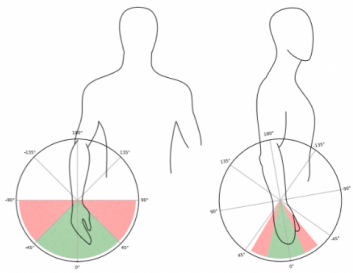

Figure 5: Ranges of conditions for hand postures: wrist extension/flexion (left) and wrist ulnar/radial deviation (right). Wrist flexion and wrist deviation color scales as Acceptable and Not Recommended.

Figure C.2: Risk assessment guidelines from ISO 11226, used in the dashboard (adapted from [97]).

Appendix D

Results and Discussion

Figure D.1: Dashboard overview and main sections.